Department of Biomedical Sciences

University of Veterinary Medicine Vienna

Institute of *in vivo* and *in vitro* Models

(Head of the Institute: Univ.-Prof. Dr. Maik Dahlhoff)

Characterisation of Mice Expressing HA-tagged *Ovol1* in the Mammary Gland

Bachelor Thesis

University of Veterinary Medicine Vienna

Submitted by

Anna Maringer

Vienna, July 2023

Supervisor:

Dr[in].rer.nat. Bettina Wagner

Univ.-Prof. Dr.med.vet. Maik Dahlhoff

Reviewer:

Dr. Jörg Burgstaller

Acknowledgements

First and foremost, I would like to thank Dr[in].rer.nat. Bettina Wagner for all the time she invested in the supervision of my work and her great support during the last months. I also thank Univ.-Prof. Dr. Maik Dahlhoff for the opportunity to work on this project.

A big thank you goes to MMag[a].rer.nat Barbara Pachner, Mag[a].med.vet. Theresa Hommel and Mag[a].med.vet. Paula Meisel who always helped me when I had questions. Furthermore, I want to thank Martin Hofer, BSc, for supporting me in performing and evaluating my qPCRs.

Thank you, Christiane, Ingo and Maria, for making it possible for me to get to this point and for supporting me in whatever I needed. And many thanks to you, Ralph, for always having my back and doing everything for me.

And to Charly, of whom I thought so often during these past months.

Table of contents

1. Introduction

1.1. Breast cancer – a worldwide problem

Breast cancer is the most common type of cancer worldwide. According to the data of the World Health Organisation (WHO) in 2020 alone almost 2.3 million women were diagnosed with breast cancer worldwide and 685,000 women died of breast cancer in that year. Almost 7.8 million women were alive by the end of 2020 that had been diagnosed with breast cancer in the five years before (Global Cancer Observatory: Cancer Today, accessed: 15/07/2023). Though the mortality rate in breast cancer is much lower than in other aggressive cancer types (R. Wang et al., 2019), metastasis is the number one cause of breast cancer deaths and tremendously affects survival rates (Boman et al., 2022; Maajani et al., 2019; R. Wang et al., 2019).

Understanding mechanisms of tumour development, growth and metastasis is inevitable for developing new ways of treatment for that kind of diseases.

1.2. Development of the mammary gland

Many different cell types are present in the mammary gland, like epithelial cells, immune cells, adipocytes, fibroblasts, lymphatic and vascular cells (Inman et al., 2015). In the epithelium two main types of cells exist, which are luminal and basal cells. The luminal cells form the ducts and secretory alveoli, the basal cells consist of myoepithelial cells. Luminal and basal cells form a bilayer that is embedded in the surrounding fat pad (Watson & Khaled, 2008).

The mammary gland's primary role is to provide food for the offspring and is the biggest difference between mammals and all other animals. Apart from nutrients in form of milk proteins and fat, the mammary gland also provides passive immunity and influences the microbiome of the progeny (Watson & Khaled, 2020). For science, the mammary gland is a great opportunity to study the development of organs since the mammary gland develops throughout the whole life of a female. Furthermore, studying the (physiological) development of the mammary gland is of great use for cancer research since many hormones and growth factors needed for mammary gland development are also present in mammary gland tumours. Many processes and pathways active in the physiological development of the mammary gland can be detected in mammary tumours as well (Inman et al., 2015; Watson & Khaled, 2008).

Also, the mammary gland can be used as a model for investigating stem or progenitor cells, the regulation of cell fate specification, the involution of a functional organ and much more.

The mammary gland develops mainly in three steps: during embryogenesis, puberty and pregnancy (Fig. 1). Many different growth factors and hormones are part of these processes.

1.2.1. Embryonic development

First, the milk lines are formed out of multi-layered ectoderm, along which five pairs of placodes develop. Buds are formed that develop to a structure consisting of five ductules, which are embedded in the subdermal fat pad. At this stage a hollow lumen is formed opening to the surface of the skin and a nipple arises. Around the ductal system white adipose tissue accumulates (Watson & Khaled, 2008).

Development of the mammary gland is arrested just before birth. Until puberty the mammary gland only grows proportionally to the body size.

1.2.2. Development during puberty

With a rise of oestrogen levels during puberty, the next development stage starts. The ductal network established during embryonic development elongates and terminal end buds (TEBs) are formed at the end of the ducts consisting of an outer layer of cap cells and a multi-layered core of body cells (Watson & Khaled, 2020). Secondary branching results from bifurcation of the ducts and lumina are formed most probably through apoptosis of the body cells (Watson & Khaled, 2008). When the mice reach adulthood a network of ducts has formed.

1.2.3. Processes during and after pregnancy

During pregnancy the mammary gland gets prepared for lactation. Alveologenesis induced by the hormones progesterone and prolactin takes place (Watson & Khaled, 2020).

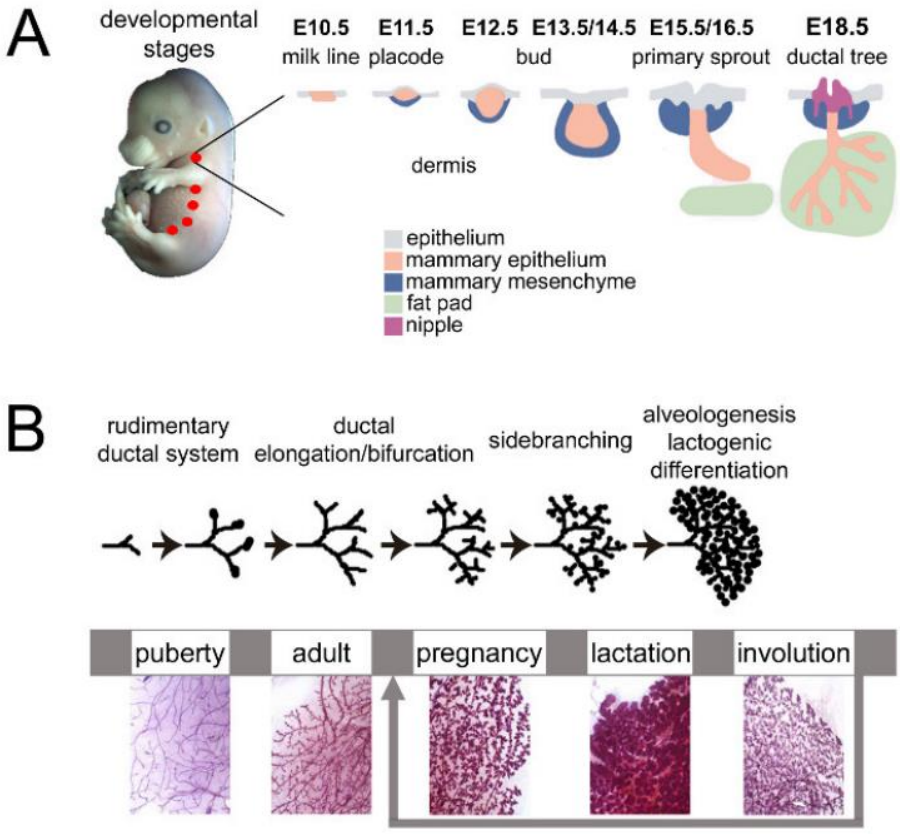

Figure 1: Development of the mammary gland (Honvo-Houéto & Truchet, 2015). A) Embryonic development of the mammary gland: First the milk lines form along which five pairs of placodes develop. Buds are formed that build a rudimentary tree with five ductules, then mammary gland development gets arrested until puberty. B) With the rise of oestrogen levels during puberty, the mammary gland development continues. Terminal end buds are formed and ducts elongate and bifurcate. During pregnancy extensive sidebranching and alveologenesis takes place. After lactation the mammary gland involutes and through cell apoptosis and tissue re-modelling an almost pre-pregnancy state is rebuilt.

Following lactation approximately 80 % of the epithelium developed during pregnancy gets removed by apoptosis and tissue re-modelling within a few days. After that process the mammary gland almost returns to a pre-pregnant state (Watson & Khaled, 2008, 2020), although the existence of an “epigenetic memory” of the mammary gland of parous mammals has been proposed, which may explain why the sidebranching and the production of milk happens faster in subsequent pregnancies (dos Santos et al., 2015). Sidebranching and cell apoptosis occur to a certain degree with every oestrus cycle throughout a female’s life (Watson & Khaled, 2008, 2020). A study suggests that the microenvironment that is generated by involution of the mammary gland after lactation can promote tumorigenesis by altering macrophage biology and lymphangiogenesis (Elder et al., 2018).

1.3. The transcription factor Ovol1 in development and disease

The mouse Ovo-like transcriptional repressor 1 (*Ovol1*) is a DNA binding protein that contains four Zinc-finger domains (Li et al., 2002). In the mouse genome two additional members of this gene family, *Ovol2* and *Ovol3* are also present (Saxena et al., 2022). OVOL1 was shown to act as a transcriptional repressor of the MYC protein (Nair et al., 2006), which enhances proliferation and stimulates cell cycle progression and, when not properly regulated, also enhances the genesis of cancer (García-Gutiérrez et al., 2019).

OVOL1 also plays an important role in epithelial lineage determination and differentiation of tissues such as skin and mammary epithelia during embryonic development and is a main actor in mesenchymal-epithelial-transition (MET). The opposite program of MET – epithelial-mesenchymal-transition (EMT) – plays a big role in invasion and metastasis of cancer by allowing epithelial cells to lose their cell-cell-adhesion and to gain motility by entering a mesenchymal state (Yang & Weinberg, 2008).

OVOL1 (as well as OVOL2) can repress EMT-inducing transcription factors to inhibit EMT. Such a transcription factor would be ZEB1. However, OVOL1 and OVOL2 are also able to promote MET by induction of E-Cadherin expression and therefore promoting cell-cell-adhesion (Roca et al., 2013). Furthermore, Jolly et al. showed a regulatory role of OVOL proteins in gaining stem cell-like characteristics, which would improve therapy-resistance and the ability to repopulate a tumour. They propose that without OVOL cells can undergo the EMT completely and gain stemness in a mesenchymal state (Jolly et al., 2015).

Due to its impact on the metastatic cascade, OVOL1 is a potential therapeutic target for treatment of (breast) cancer. However, some studies also show a contributing role of MET in the formation of secondary tumours which should be kept in mind when thinking of suppressing EMT or promoting MET as a treatment against cancer (Chaffer et al., 2006; Roca et al., 2013).

Though there are many studies investigating the role of OVOL1 in certain pathways that may contribute to the development of cancer conducted in cell lines, studying the role of OVOL1 in a mouse model may help to clarify open questions regarding the effects of OVOL1 on mammary gland tumours.

1.4. A mouse model for mammary gland specific expression of OVOL1

Animal models to study diseases should reproduce the causes of development, biological behaviour, pathology, and the response to therapeutics as well as possible. For breast cancer mostly rodents are used as animal model. Mice show similarities to human genetics, have a short generation cycle and are – compared to other lab animals – relatively cheap (Zeng et al., 2020). For a study of OVOL1 in mammary tumours currently conducted at the Institute for *in-vivo* and *in-vitro* Models at the University for Veterinary Medicine Vienna a transgenic mouse line overexpressing OVOL1 should be established.

For establishing such a line, first a construct containing the haemagglutinin (HA)-tagged coding sequence (CDS) of mouse *Ovol1* under the control of the Mouse Mammary Tumour Virus (MMTV)-Promoter was generated. An HA-tag was inserted at the N-terminal end of the *Ovol1*-CDS by PCR. The HA-tagged *Ovol1*-CDS was inserted into an *EcoR*I restriction site that is located after the MMTV-Promoter (Fig. 2). The construct also contains a Simian Virus (SV) 40 nuclear localisation site (NLS), a small-t intron and a SV40 polyadenylation (poly A) sequence.

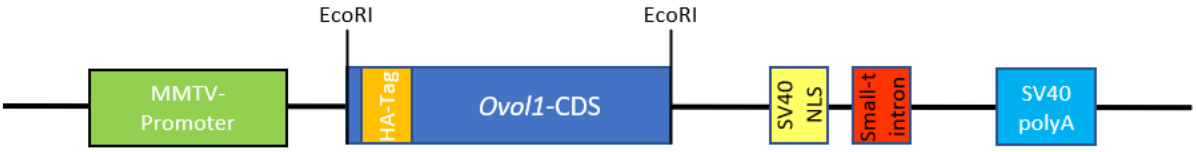

Figure 2: Construct for generating MMTV-HA-Ovol1 transgenic mice. The Mouse Mammary Tumour Virus Promoter induces the expression of the transgene Ovol1 which is tagged with an HA-tag at the N-terminal side for detection. The SV40 nuclear localisation sequence (NLS) allows the construct to enter the nucleus. The small-t intron max promote transgene expression by increasing the translation efficiency. The SV40 polyadenylation sequence (polyA) signals the end of the transcript. The HA-tagged Ovol1-CDS was inserted into an EcoRI recognition site.

The MMTV-Promoter is a well-established promoter to direct gene expression to the mammary gland. It has been used to generate various mouse models for mammary gland development and disease (Taneja et al., 2009; Wagner et al., 2001). Activity of the MMTV-Promoter is regulated by binding of the progesterone receptor (Beato et al., 2020).

The HA-tag was introduced to facilitate detection of OVOL1 expression. The HA-tag is a short epitope tag which is often attached to uncharacterized proteins, to allow detection if antibodies against that protein have not yet been developed (Zhao & Méresse, 2015).

Mice transgenic for MMTV-HA-Ovol1 were then generated by pronucleus injection. The transgenic construct is microinjected into one-cell stage zygotes and randomly integrates into the genome. With this technique transgenes can be efficiently introduced into the mouse

genome. However, a few specifics of these technique need to be taken into consideration. DNA integration may occur after the one cell stage and founder mice will be mosaic for the integration. The transgene may integrate into multiple chromosomal sites in the founder mice. Transgene expression is not only dependent on the activity of the transgenic promoter but is also influenced by the integration locus. Depending on the integration locus the transgene can be epigenetically modified which could alter gene expression and transgenes at different integration sites may be differently expressed (Allen et al., 1990; Rülicke & Hübscher, 2000). Therefore, multiple transgenic integrations need to be separated from each other in order to obtain a line with a constant transgene expression. Mice with a stable transgene integration will transmit the transgene at Mendelian ratios to their offspring (Rülicke & Hübscher, 2000). For using transgenic mice in consecutive experiments, a stable and consistent transgene expression is required.

A stably expressing MMTV-HA-Ovol1 line will be crossed into another genetically modified mouse model that develops mammary gland cancer to clarify the role of OVOL1 in breast cancer development.

1.5. Aim of the thesis

To study the role of OVOL1 *in vivo* finding a suitable animal model is inevitable. For this, biochemical and molecular biological tests must be performed to ensure, that the chosen mouse model will be suitable for the planned projects. Aim of this thesis is to examine the transcription, by qPCR, and the translation, by Western Blot analysis, of mammary gland specific OVOL1 in the mouse lines generated with pronucleus injection.

In the end a data set should be generated, which helps to identify a mouse line with a stable overexpression of OVOL1 in the mammary gland.

2. Material & Methods

2.1. Material

2.1.1. Reagents and Kits

- Proteinase K, EO0492, Thermo Fisher Scientific, USA
- DNeasy Blood & Tissue Kit, QIAGEN GmbH, Germany
- Monarch Total RNA Miniprep Kit, T2010, New England Biolabs, USA
- DNase I Reaction Buffer, B0303, New England Biolabs, USA
- DNase I, M0303, New England Biolabs, USA
- LunaScript RT SuperMix Kit, E3010, New England Biolabs, USA
- One*Taq* DNA Polymerase, M0480, New England Biolabs, USA
- dNTP Set, R0181, Thermo Fisher Scientific, USA
- GelRed Nucleic Acid Stain, 41003, Biotium, USA
- Agarose, A9539, Sigma-Aldrich, Germany
- Rotiphorese 50x TAE Puffer, CL86.1, Carl Roth GmbH + Co KG, Germany
- GeneRuler 100 bp Plus DNA Ladder, SM0322, Thermo Fisher Scientific, USA
- One*Taq* Quick-Load 2X Master Mix with Standard Buffer, M0486, New England Biolabs, USA
- Luna Universal qPCR Master Mix, M3003, New England Biolabs, USA
- Protease Inhibitor Cocktail, 8340, Sigma-Aldrich, Germany
- Glycerol, G5516, Sigma-Aldrich, Germany
- Triton X-100, T9284, Sigma-Aldrich, Germany
- Albumin Standard, 23209, Thermo Scientific, USA
- Pierce™ Detergent Compatible Bradford Assay Reagent, 23246, Thermo Fisher Scientific, USA
- PageRuler™ Prestained Protein Ladder, 10 to 180 kDa, #26616, Thermo Fisher Scientific, USA
- OVOL1 Rabbit Polyclonal antibody, 14082-1-AP, proteintech, USA
- HA-Tag (C29F4) Rabbit mAb, #3724, Cell Signaling Technology, USA
- β-Tubulin (D2N5G) Rabbit mAb, #15115, Cell Signaling Technology, USA
- Anti-rabbit IgG, HRP-linked Antibody, #7074, Cell Signaling Technology, USA
- Clarity Western ECL substrate, 170-5060, BioRad, Germany
- Amersham™ Hybond® P Western blotting membranes, PVDF, 0.45 µm, GE10600023, Sigma-Aldrich, Germany

- Extra Thick Blot Filter Paper, Precut, 15 x 20 cm #1703960, BioRad, Germany
- EMSURE® ACS, ISO, Reag. Ph. Eur. zur Analyse, Methanol ≥99.9%, 1.06009, Supelco®, Merck, Germany
- TEMED, A1148,0025, PanReac AppliChem, Germany
- Ethanol Absolut 99.9 %, AustrAlco, Austria
- Ethanol ≥70 %, denatured, Carl Roth GmbH + Co KG, Germany
- RNase-free water, W4502-1L, Sigma-Aldrich, Germany

2.1.2. Buffer & Solutions

- TNES-Buffer (10 mM Tris-Cl pH 7.5, 400 mM NaCl, 100 mM EDTA, 0.6 % SDS)
- TE-Buffer (1 M Tris-HCl pH 7.5, 500 mM EDTA)
- 1 M Hepes-Buffer pH 7.3
- 1 M $MgCl_2$, M1028, Sigma-Aldrich, Germany
- 500 mM EGTA pH 8
- 0.1 % Ponceau S solution
- TBS 10x (200 mM Tris, 1.5 M NaCl)
- TBS-T (20 mM Tris, 0.15 M NaCl, 0.05 % Tween20)
    - Tween20, P9416, Sigma-Aldrich, Germany
- Milk Blocking buffer
    - Difco™ Skim Milk, 232100, Becton, Dickinson and Company, France
- 4x Laemmli sample buffer (200 mM Tris-HCl pH 6.8, 8 % SDS, 40 % Glycerol, 20 % β-mercaptoethanol)
- 10 % APS
- 30 % Acrylamide
- Separating Gel Buffer 4x (1.5 M Tris-HCl, pH 8.8, 0.4 % SDS)
- Stacking Gel Buffer 4x (0.5 M Tris-HCl, pH 6.8, 0.4 % SDS)

2.1.3. Equipment

- Intas Gel iX Imager, Intas Science Imaging Instruments GmbH, Germany
- multiSUB Choice, Wide Midi Horizontal Electrophoresis System, Cleaver scientific LTD, United Kingdom
- peqSTAR 2X Thermocycler, PQ95-07002, peqlab, Germany
- Biometra TAdvanced, Analytik Jena, Germany
- Mini-Sub Cell GT, BioRad, Germany
- PowerPac™ Basic Power Supply, Bio-Rad Laboratories GmbH, Germany

- qTOWER^3 G, Analytik Jena, Germany
- BioPhotometer, #6131, Eppendorf, Germany
- LabelGuard™ Microliter Cell with 0.2 mm lid, Implen, Germany
- DPU-414 Thermal Printer, Seiko Instruments Inc., Japan
- Miccra MiniBatch D-1 homogeniser, DS-5-PE dispersing tool, Miccra GmbH, Germany
- HANNA pH 213, Microprocessor pH Meter, USA
- Sunrise Absorbance Reader, TECAN Trading AG, Switzerland
- Rocking Platform, VWR, USA
- Trans-Blot Turbo Transfer System, BioRad, Germany
- PowerPac HC, BioRad, Germany
- Mini-PROTEAN Tetra Cell, BioRad, Germany
- Fusion FX, Vilber Lourmat, France
- HERMLE, Z 326 K, HERMLE Labortechnik GmbH, Germany

- Centrifuge 5910 R, Eppendorf, Germany
- Centrifuge 5810 R, Eppendorf, Germany
- Centrifuge 5415 R, Eppendorf, Germany
- Mini centrifuge Sprout plus, Carl Roth GmbH + Co KG, Germany
- Color Sprout Plus Mini-Centrifuge, Biozym Scientific GmbH, Germany
- Thermomixer compact, Eppendorf, Germany
- Vortex-Genie™ 2, Scientific Industries SI™, Germany
- peqTWIST, peqlab, Germany
- MS3 basic, IKA-Werke GmbH & CO. KG, Germany
- KERN EG220-3NM, Kern & Sohn GmbH, Germany
- RAININ Pipet-Lite XLS, Mettler Toledo, USA
- Eppendorf research plus, Eppendorf, Germany

2.1.4. Software

- Intas GDS Touch 2, Intas Science Imaging Instruments GmbH, Germany
- qPCRsoft, Software version 4.1, Analytik Jena, Germany
- Magellan, Software version 7.3, TECAN Trading AG, Switzerland
- Evolution-Capt, V18-03, Vilber Lourmat, France

2.1.5. Plastic consumables

- RAININ BioClean Ultra™, Mettler Toledo, USA; 10 µl, 200 µl and 1000 µl
- SafeSeal SurPhob Spitzen, Biozym Biotechnologie GmbH, Germany; 10 µl, 300 µl and 1250 µl
- Micro tube 2.0 ml SafeSeal, DNA-/DNase-/RNase-/PCR inhibitor-free, SARSTEDT AG & Co. KG, Germany
- Micro tube 1.5 ml SafeSeal, DNA-/DNase-/RNase-/PCR inhibitor-free, SARSTEDT AG & Co. KG, Germany
- Micro tube 5.0 ml PCR-PT, DNA-/DNase-/RNase-/PCR inhibitor-free, SARSTEDT AG & Co. KG, Germany
- Multiply®-Pro mix. Colour, DNA-/DNasse-/RNase-/PCR inhibitor-free, SARSTEDT AG & Co. KG, Germany
- 8-Lid chain, flat, 65.989.002, SARSTEDT AG & Co. KG, Germany
- Multiply®-µStrip 0.2 ml chain, 72.985.002, SARSTEDT AG & Co. KG, Germany
- 96 Well PCR Platte, weiß, LC 480, DNA-, DNase, RNasefrei, 710877, Biozym Scientific GmbH, Germany
- Expell™ PCR 96 & 384-well optical sealing membrane, sticky adhesive, 5100402C, CAPP, AHN Biotechnologie GmbH, Germany
- PCR-plate PP, 384x40µl, full-skirted, white, 04-083-0384, nerbe plus GmbH & Co. KG, Germany

2.1.6. Primers

Primers were synthetised as standard desalted DNA oligonucleotides by Sigma-Aldrich, Germany. Primer designations, sequences and intended use are listed in Table 1.

MMTV-HA_Ovol1 genotyping primers were designed using the freely available software ApE (https://jorgensen.biology.utah.edu/wayned/ape/). Primer sequences for Ornithine decarboxylase antizyme 1 (*Oaz1*) were provided by Ralf Steinborn (VetCore). Primers for *Ovol1* were designed by IDT (Integrated DNA Technologies, Inc., USA) and primers for Beta-2-microglobulin (*B2m*) were selected from the database PrimerBank (X. Wang et al., 2012).

Table 1: Primers used in PCR reactions throughout the experiments

Purpose	Primer	Sequence
Genotyping (transgene)	*MMTV_Ovol1_geno_fw4*	5'-TGGACATGAGCCTTCGAGAC-3'
Genotyping (transgene)	*MMTV_Ovol1_geno_rev3*	5'-TGACTCTCGGATGTGCAACC-3'
Genotyping (control PCR)	*CSD-Ovol1-F*	5'- AGAGGTGGGCAGATTTCTGAGTTCC-3'
Genotyping (control PCR)	*CSD-Ovol1-ttR*	5'- AAGCCATTAAGCTACATTGCCAGCC-3'
qPCR (Reference gene)	*Oaz_QPCR_fw_1*	5'-GTGGTGGCCTCTACATCGAG-3'
qPCR (Reference gene)	*Oaz_QPCR_rev_1*	5'-AGCAGATGAAAACGTGGTCAG-3'
qPCR (gene of interest)	*Ovol1_E2-3_fw*	5'-AGCTACCCTCTGAAGATGTGA-3'
qPCR (gene of interest)	*Ovol1_E2-3_rev*	5'-GTGAAGGACTTCTGGCAGATG-3'
qPCR (Reference gene)	*B2m_qPCR_fw3*	5'-TTCTGGTGCTTGTCTCACTGA-3'
qPCR (Reference gene)	*B2m_qPCR_rev3*	5'-CAGTATGTTCGGCTTCCCATTC-3'

2.1.7. Tissue samples

Several samples used during my project were initially generated for other projects and kindly provided by colleagues. These samples are listed in Table 2 and Table 3.

Table 2: Samples from experimental animals

Animal number	Mouse line	Tissue source	Type of sample	genotype	Contributed by
0421-0481	B6;Cg-Ovol1^{tm1c}-Tg(MMTV-Cre)4Mam	mammary gland, kidney	frozen tissue	Ovol1 flox/flox	Bettina Wagner
0421-0488	B6;Cg-Ovol1^{tm1c}-Tg(MMTV-Cre)4Mam	mammary gland	frozen tissue	Ovol1 flox/flox, MMTV-Cre T/+	Bettina Wagner
0342-0222	C57BL/6-Elovl7$^{tm1a(EUCOMM)Hmgu}$	testis, liver	protein lysate	+/+	Hannah Schröder
1239-0053	B6129-Tgn(MMTV-Cre)4Mam	liver, kidney, testis, skin, lung, heart, cortex, cerebellum, spleen	RNA	+/+	Hannah Schröder

Table 3: Cell lysates

Sample	Protein concentration sample [µg/µl]	Contributed by
HEK293 control	4.0	Bettina Wagner
HEK293 CHA-Ing3	3.4	Bettina Wagner
HEK293 NHA-Ing3	3.2	Bettina Wagner
NIH3T3 LRIG2	14.5	Theresa Hommel

2.1.8. Animals

MMTV-HA-Ovol1 transgenic mice were generated by pronuclear injection at the Institute of *in vivo* and *in vitro* Models (animal experimentation license number: BMBWF-68.205/0010-V/3b/2019). Three MMTV-HA-Ovol1 transgenic founder mice were identified and the offspring of each founder were treated as a separate line (C57BL/6N-Tg(MMTV_HA_Ovol1)796Biat, C57BL/6N-Tg(MMTV_HA_Ovol1)797Biat, C57BL/6N-Tg(MMTV_HA_Ovol1)798Biat). Subsequently these lines will be referred to as L796, L797 and L798.

To identify mice carrying a stable transgene integration, transgenic males from each line were backcrossed to C57BL/6N females. In this setting animals carrying a stable transgenic integration should transmit the transgenic allele to 50 % of their offspring. Offspring from animals with a higher transgene transmission rate were not further considered in the current analysis.

Mice were housed in specific pathogen-free conditions in accordance with FELASA recommendations (Mähler et al., 2014). Regular mouse diet and water were provided *ad libitum*. Mice were kept in individually ventilated cages with a maximum of five mice per cage. Adequate enrichment and nesting material were provided in each cage. The surrounding temperature and the relative humidity (temperature: 22 °C ± 1 °C; relative humidity: 50 % ± 10 percentage points) were monitored and regulated. Animal handling and health monitoring was performed by trained animal caretakers and the scientific investigators.

At weaning age (day 17 – 21 after birth) ear notching was performed for subsequent identification of the animals. From each mouse an ear biopsy was collected and was further used as tissue sample for genotyping.

2.2. Methods

2.2.1. Preparation of genomic DNA from mouse tissue samples

Ear biopsies were used as source of DNA for genotyping. For re-genotyping of sacrificed mice tail tissue was used for DNA preparation.

DNA was prepared according to the following procedure:

100 µl TNES-Buffer and 2 µl Proteinase K were added to each tissue sample. The samples were then incubated at 55 °C overnight. 35 µl 5 M NaCl were added to the sample and the

sample was incubated on a thermomixer at 1400 rpm. Tubes were then centrifuged at 13,000 rpm and 100 µl supernatant was transferred into new microfuge tubes. 100 µl cold 100 % ethanol was added to precipitate the DNA and the samples were centrifuged at 13,000 rpm to pellet the precipitate. Supernatant was aspirated, the pellets were washed with 70 % ethanol and then air dried before dissolving the pellet in 100 µl TE-Buffer.

For some samples tails of sacrificed mice were used to repeat DNA preparation with the DNeasy Blood & Tissue Kit according to the manufacturers protocol. After the tissue was lysed, the samples were centrifuged, and the supernatant was put into a new microcentrifuge tube to get rid of the hair in the sample to prevent clogging of the spin column. In the end the DNA was eluted twice in 100 µl Buffer AE.

Genomic DNA samples were stored at 4 °C until genotyping.

2.2.2. Genotyping

To determine whether the mice carried the MMTV-HA-Ovol1 transgene they were genotyped by PCR which was performed under the following conditions:

Table 4: Master Mix for the genotyping PCR to detect the transgene

Reagent	Final concentration
One*Taq* Standard Buffer	1 ×
dNTP Mix	0.2 mM
MMTV_Ovol1_geno_fw4	0.25 µM
MMTV_Ovol1_geno_rev3	0.25 µM
One*Taq* DNA Polymerase	1 U
Nuclease free H_2O	

PCR reactions were performed in a final volume of 20 µl using 1 µl of genomic DNA.

Table 5: Thermocycler conditions for the genotyping PCR to detect the transgene

Temperature	Duration	
94 °C	2 minutes	
94 °C	15 seconds	35 cycles
62 °C	20 seconds	
68 °C	30 seconds	
68 °C	2 minutes	

Using the *MMTV_Ovol1_geno_fw4/MMTV_Ovol1_geno_rev3* primer pair (Tab. 1) a 493 bp fragment will be amplified from MMTV-HA-Ovol1 transgenic mouse DNA. The corresponding wildtype fragment has a size of 2602 bp and should not be amplified using the PCR cycling conditions described above. However, in some cases the wildtype fragment could be detected.

To check whether it is possible to amplify a PCR fragment from the mouse genomic DNA samples a control PCR was performed under the following conditions:

Table 6: Master Mix for the control PCR

Reagent	Final concentration
One*Taq* Standard Buffer	1 ×
dNTP Mix	0.2 mM
CSD-Ovol1-F	0.15 µM
CSD-Ovol1-ttR	0.15 µM
One*Taq* DNA Polymerase	1 U
Nuclease free H_2O	

PCR reactions were performed in a final volume of 20 µl using 1 µl of genomic DNA.

Table 7: Thermocycler conditions for the control PCR

Temperature	Duration	
94 °C	2 minutes	
94 °C	15 seconds	35 cycles
65 °C	20 seconds	
68 °C	30 seconds	
68 °C	2 minutes	

PCR fragments were analysed by agarose gel electrophoresis, using a 1 % agarose gel. 15-20 µl of each sample mixed with loading dye and 3-5 µl GeneRuler 100 bp Plus DNA Ladder were loaded per well respectively. The amount of sample and DNA ladder loaded depended on the width of the wells.

The results of the genotyping PCRs were used for calculating the number of transgenic versus wildtype offspring and selecting the females for tissue preparation.

2.2.3. Tissue preparation

For tissue preparation eight to ten weeks old female mice were sacrificed by cervical dislocation. The mice were weighed and checked for any abnormalities. Mice showing

abnormalities (e.g., overgrown teeth) were not included in the analysis. Tissue samples were harvested immediately after sacrificing the animal according to the procedure described below.

First, an incision was made into the abdominal skin and the cut was extended towards the chin and the pubis of the mouse. The abdominal skin was pulled away from the peritoneum and fixed with several needles on both sides of the mouse. Then the abdominal and thoracal mammary glands (Fig. 3) were harvested. To prepare the reproductive organs first the abdominal musculature was removed and the pubic bone was cut with scissors. The ovary and the uterus were carefully cleared from fat tissue. The whole reproductive apparatus containing the ovaries, uteri and the cervix was pulled out of the abdominal cavity and an incision was made at the transition from cervix to vagina. The kidney and the liver were removed and carefully cleared from as much unwanted tissue (e.g., fat) as possible. The thoracic cavity was opened and the heart was dissected. Finally, a piece of shaved skin was removed from the back of the mouse. The tissue samples were cut into small pieces and transferred to DNase-/RNase-free microfuge tubes. To avoid degrading of the RNA, samples were immediately frozen in liquid nitrogen and then stored at -80 °C.

In addition, a tail sample from each mouse was stored at -20 °C.

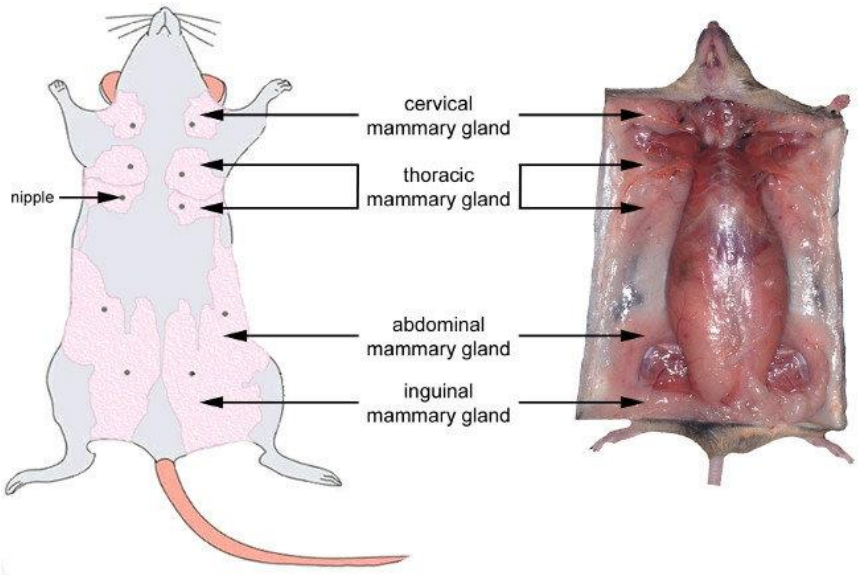

Figure 3: Position of the mammary glands in mice (Honvo-Houéto & Truchet, 2015); for the experiments the thoracic and abdominal mammary gland were prepared.

2.2.4. RNA preparation

RNA was prepared from abdominal mammary gland tissue of transgenic as well as wildtype animals. RNA preparation was performed using the Monarch Total RNA Miniprep Kit (#T2010, New England Biolabs) according to the manufacturers protocol. The tissue samples first were homogenized using the Miccra MiniBatch D-1 homogeniser with the DS-5-PE dispersing tool in DNA/RNA protection reagent. Samples then were incubated with Proteinase K for 5 minutes at 55 °C. Afterwards samples were centrifuged, and the supernatant was transferred to a clean DNA-/RNA-free microfuge tube. The supernatant was mixed with Lysis Buffer, transferred to a gDNA Removal Column fitted with a collection tube and centrifuged to remove most of the genomic DNA. Ethanol was added to the flow-through. The mixture was transferred to an RNA Purification Column again fitted with a collection tube. Samples were centrifuged to remove all liquids. To remove residual genomic DNA, DNase I treatment was performed by adding DNase I onto the column and by incubating the reaction for 15 minutes at room temperature. After DNase I treatment, RNA Priming Buffer was pipetted in the column followed by centrifugation and two washing steps. Lastly, the RNA Purification Column was transferred to an RNase-free Microfuge Tube and RNA was eluted in nuclease-free water.

Due to the difficult nature of the mammary gland tissue a few adaptations to the described protocol were made:

First, a higher amount of protection reagent than recommended in the manual was used for homogenisation. Following centrifugation of the homogenised sample, no defined pellet could be detected at the bottom of the tube, but instead a thin white fat layer formed on the surface of the lysate. For transferring the homogenate containing the RNA to another reaction tube it was necessary to avoid transferring too much of this fat layer. Contamination of the homogenate with the fat layer led to poorer results as far as RNA purity and concentration were concerned. It turned out that by using more of the protection reagent the quality of the RNA samples could be increased.

Second, to ensure that all liquid was removed from the columns the reaction tubes were always centrifuged for 1 minute instead of 30 seconds.

Furthermore, since concentration determination of the first samples showed rather low RNA-concentrations the RNA elution volume was reduced from 100 to 50 µl.

The concentration of the RNA was measured with the Eppendorf BioPhotometer using the LabelGuard™ Microliter Cell with a 0.2 mm lid and 2 µl RNA sample. For determination of the

RNA concentration the absorbance was measured at a wavelength of 260 nm. As indicators for purity of the RNA, absorbance at 230, 280 and 320 nm were measured as well. For further experiments the results calculated by the Eppendorf BioPhotometer were used.

The RNA samples were stored at -80 °C.

2.2.5. cDNA synthesis

To investigate gene expression by RT-PCR it is first necessary to produce complementary DNA (cDNA) from RNA.

For cDNA synthesis the LunaScript RT SuperMix Kit was used. This kit includes a master mix, the LunaScript RT Supermix (5x) which contains all components required for generating cDNA and a No-RT control Mix (5x). Up to 1 µg of RNA can be transcribed in one reaction.

The amount of RNA sample needed for the reaction depended on the concentration in the sample; in the final cDNA sample (total volume 20 µl) the amount of RNA should be 600 ng (30 ng/µl).

The cDNA synthesis was performed in a thermocycler according to the following protocol:

Table 8: Thermocycler programme for cDNA synthesis

Temperature	Duration	
25 °C	2 minutes	1 cycle
55 °C	10 minutes	
95 °C	1 minute	

2.2.6. DNase I treatment

To remove as much left-over genomic DNA as possible since too much remaining genomic DNA would confound the results of the (q)RT-PCR RNA samples were treated with DNase I for qPCR according to the following protocol:

Table 9: Protocol for DNase I treatment of RNA samples

Reagent	µl
RNA	
10x DNase I Buffer	2.5
DNase I	1
H_2O	

The total volume of the reaction was 25 µl.

The samples were incubated at 37 °C for 10 minutes followed by the inactivation of DNase I by heating it up to 95 °C for 5 minutes.

2.2.7. RT-PCR

RT-PCR was performed to initially test primers for subsequent qPCR and to determine *Ovol1* expression levels in different tissue types.

RT-PCRs were performed under the following conditions:

Table 10: RT-PCR Master Mix

Reagent	Final concentration
One*Taq* 2x Master Mix	1 ×
Primer forward	0.5 µM
Primer reverse	0.5 µM
Nuclease free H_2O	

The total volume of each reaction was 20 µl using 1 µl of cDNA. The RT-PCR for the reference gene was done using a 1:100 dilution of the cDNA as template. Primers used for RT-PCR are described in Tab. 1.

Table 11: PCR protocol for RT-PCR

Temperature	Duration	
94 °C	2 minutes	
94 °C	15 seconds	35 cycles
60 °C	15 seconds	
68 °C	15 seconds	
68 °C	2 minutes	

The results were visualized by performing gel electrophoresis using a 2 % agarose gel.

2.2.8. Quantitative PCR (qPCR)

To determine the amount of *Ovol1* expression in mammary gland tissue qPCRs were performed.

qPCRs were performed at the VetCore facility (University of Veterinary Medicine, Vienna) using the qTOWER^3 G instrument (for 96 well plates).

qPCR was performed for *Ovol1* as well as the reference genes Beta-2-microglobulin (*B2m*) and Ornithine decarboxylase antizyme 1 (*Oaz1*). All samples and standards were measured in triplicates. A standard curve and a no template control were included in each run.

For each gene an according assay with the following primer pairs were used:

For *Ovol1*: *Ovol1_E2-3_fw/Ovol1_E2-3_rev*
For *Oaz1*: *Oaz_QPCR_fw_1/ Oaz_QPCR_rev_1*
For *B2m*: *B2m_qpcr_fw3/B2m_qpcr_rev3*

Table 12: qPCR Master Mix

Reagent	Final concentration
Luna Universal qPCR Master Mix	1 ×
Primer forward	0.125 µM
Primer reverse	0.125 µM
Nuclease free H_2O	

The final volume per reaction was 20 µl, using 2 µl cDNA.

qPCR was performed under the following conditions:

Table 13: qPCR Protocol

Temperature	Duration	
95 °C	1 minute	
95 °C	15 seconds	40 cycles
60 °C	15 seconds	

Additionally, a melting curve was generated to evaluate whether the correct cDNA fragment was amplified based on its melting temperature. Measurements started at 60 °C for 35 loops. With every loop the temperature was raised by 1 °C.

At the end of the run several parameters were calculated by the analysis software. These parameters were the individual Cq value for each well, the mean Cq value for each triplicate and the standard deviation for each triplicate. The analysis software also generates a standard curve based on the Cq values of the standard samples and calculates its amplification efficiency and its coefficient of determination. Melting curve analysis is also performed by the software.

Evaluation of a qPCR experiment was performed according to the following criteria. The amplification efficiency of the standard curve is higher than 85%. No template controls do not show a measurable Cq value. The standard deviation of the Cq values for a sample calculated by the software is below 0.5. Samples with a standard deviation above 0.5 were excluded from the analysis.

Calculation of the relative Ovol1 expression levels was performed using the following approach. The average of mean Cq values is calculated for the control group for each target gene. The relative quantity (2^{DCq}) of each sample is calculated for each target gene. The relative quantity of Ovol1 is normalised to the geometric mean of the relative quantities for *B2m* and *Oaz1.* Then the average relative normalized expression of each biological group is calculated (Taylor et al., 2019).

2.2.9. Preparation and concentration measurement of protein samples

Protein was isolated from abdominal mammary gland tissue samples according to the following procedure. Complete protein lysis buffer was prepared by diluting protease inhibitor 1:100 in protein lysis buffer (50 mM Hepes-Buffer pH 7.3, 150 mM NaCl, 10 % glycerol, 1.5 mM $MgCl_2$, 1 % Triton X-100, 1 mM EGTA ph 8). The frozen tissue sample was transferred to a 2 ml reaction tube and complete protein lysis buffer was added to the sample. The amount of complete protein lysis buffer used was estimated according to the size of the tissue sample. The tissue was homogenised using the Miccra Mini Batch D-1 homogeniser with the DS-5-PE dispersing tool. Homogenates were incubated on ice for 30 minutes and then centrifuged at 16,000 rpm for 10 minutes. The supernatant containing the protein lysate was transferred into a new tube. The protein samples were stored at -80 °C.

Determination of protein concentration

For subsequent Western Blot analysis the protein concentration in the lysates had to be determined. Concentration determination was performed using the Pierce™ Detergent Compatible Bradford Assay Reagent Kit.

To set up a standard curve Bovine Serum Albumin (BSA) supplied with the kit (concentration 2 mg/ml) was diluted in lysis buffer to final concentrations of 50, 100, 200, 300 and 400 µg/ml. A sample containing only lysis buffer was used as blank. Protein lysates were prediluted in lysis buffer at ratios between 1:5 and 1:50.

BSA standards, protein lysates and the blank were transferred to a 96 well microplate and mixed with the assay reagent at a ratio of 1:30. All samples were incubated at room temperature for 10 minutes and the absorbance was measured at a wavelength of 595 nm in the Sunrise absorbance reader using the Magellan™ software. BSA standards and protein lysates were measured as duplicates.

The blank value was subtracted from all other individual sample and standard replicates. A standard curve was prepared by plotting the average of each standard measurement versus its concentration in Microsoft Excel. Microsoft Excel was used to compute a regression line. The concentration of the protein lysates was calculated using the linear equation of the regression line (Fig. 4).

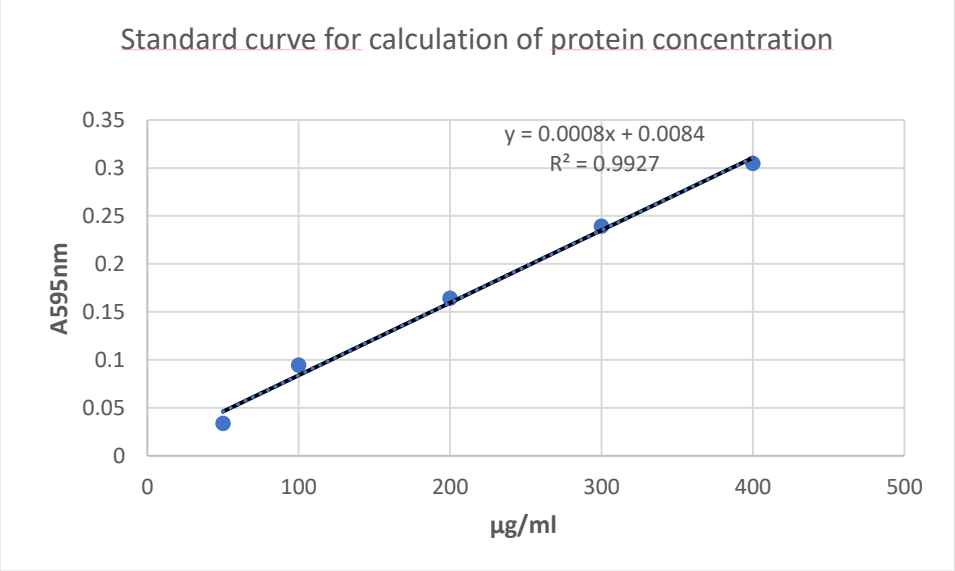

Figure 4: Example for a standard curve for calculation of protein concentration. BSA standards were measured at concentrations of 50, 100, 200, 300 and 400 µg/ml. Concentration of the samples were then calculated with the linear equation of the drawn regression line.

2.2.10. Western Blot

Polyacrylamide gel electrophoresis was performed using the Mini-PROTEAN Tetra Vertical Electrophoresis system using 1 mm handcast gels. Gels were cast in the Mini-PROTEAN Tetra Cell Casting Module according to the following protocol. After assembly of the Casting Module the separating gel was prepared as described in Table 14. Two separating gels can be prepared from 10 ml of separating gel solution.

Table 14: Composition of a 10 % separating gel solution (10 ml)

Separating Gel Buffer (4x)	2.5 ml
dd H_2O	4.2 ml
Acrylamide 30 %	3.3 ml
10 % APS	100 µl
TEMED	10 µl

Since APS and TEMED initiate polymerisation of acrylamide both components were added right before pipetting the solution into the gel mould. The mixture was pipetted into the gel mould and covered with approximately 400 µl isopropanol. When the separating gel had completely polymerized the isopropanol was decanted and the remaining isopropanol was removed with filter paper without touching the gel surface.

The stacking gel was prepared as described in Table 15 and filled into the mould up to the edge of the lower front plate. Finally, a comb with 15 lanes was inserted.

Table 15: Composition of a 3.75 % stacking gel solution (5 ml)

Stacking Gel Buffer (4x)	1.25 ml
dd H_2O	3.13 ml
Acrylamide 30 %	0.63 ml
10 % APS	50 µl
TEMED	7.5 µl

After polymerization of the stacking gel, gels were either used immediately or were wrapped in damp cloths and stored in the refrigerator at 4 °C.

Sample preparation:

Samples for Western Blot were prepared as follows:

The samples were diluted with 4x Laemmli sample buffer and complete protein lysis buffer. For tissue samples derived from MMTV-HA-Ovol1 mice a final volume of 20 µl was prepared. For protein lysates from HEK293 cell lines and from NIH3T3 cells, as well as from tissue samples from other mouse lines (see Tab. 2), a final volume of 16 µl was prepared. For tissue samples 10 µg, for HEK293 cell lines 2 µg and for NIH3T3 20 µg protein was loaded.

Following preparation samples were incubated at 95 °C in a thermomixer for 10 minutes.

Electrophoresis:

For electrophoresis two gels were placed in the clamping frame and transferred to the Mini Tank of the Mini-PROTEAN Tetra Cell. 1x Running buffer was prepared from a 10x stock solution and filled into the electrophoresis tank.

Table 16: Composition of 10x Running Buffer

10x Running Buffer
250 mM Tris
1.9 M Glycin
35 mM SDS

The gels were loaded with 16 µl sample (or 20 µl in case of samples derived from MMTV-HA-Ovol1 mice) and 5 µl Marker (PageRuler™ Prestained Protein Ladder, 10 to 180 kDa) per well respectively. The electrophoresis system was connected to a PowerPac HC power supply and the current was set to 50 V until the samples reached the separating gel. Then the current was adjusted to 100 V until the visible running front left the gel.

Blotting:

After electrophoresis a semidry transfer to Polyvinyliden fluorid (PVDF) membranes with a discontinuous buffer system (Tab. 17) was performed using the Trans-Blot Turbo Transfer System.

Table 17: Buffers for protein transfer to a PVDF membrane

Membrane Buffer for PVDF	
Tris base	47.9 mM
Glycin	35.7 mM
Methanol	16 %
H_2O	

Gel Buffer for PVDF	
Tris base	47.9 mM
Glycin	35.7 mM
10 % SDS	0.4 %
H_2O	

Two filter papers were prepared for each membrane, one soaked in gel buffer for the top and one soaked in membrane buffer for the bottom of the blotting sandwich.

Membranes were activated in methanol for 5 minutes. The blotting sandwich was assembled (Fig. 5). The preprogramed protocol “StandardSD” of the Trans-Blot Turbo Transfer System (BioRad, Germany) was used for transfer (30 minutes with 25 V).

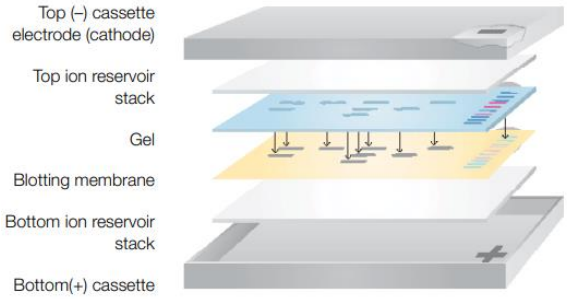

Figure 5: Blotting sandwich scheme for semidry transfer on PVDF membranes (Trans-Blot Turbo Transfer System Instruction Manual, Catalog #1704150)

After blotting the membranes were again activated in methanol for 2 minutes shaking.

The membranes were stained in 0.1 % Ponceau S solution for 1 minute shaking and a picture was taken. Then the membranes were washed with ddH_2O for another minute to remove the staining.

Immunodetection:

For immunodetection TBS-T was prepared by diluting a 10x stock solution of TBS and adding 500 µl Tween20.

The membranes were blocked in blocking buffer (5 % skim milk in TBS-T) for 1 hour at room temperature on a shaker.

The following primary antibodies were used: OVOL1 Rabbit Polyclonal antibody, HA-Tag (C29F4) Rabbit mAb and β-Tubulin (D2N5G) Rabbit mAb. As secondary antibody Anti-rabbit IgG, HRP-linked Antibody was used.

The primary antibodies were diluted 1:1000 in blocking buffer and the membranes were incubated in the primary antibody solution at 4 °C overnight on a shaker.

After overnight incubation the membranes were washed three times for 10 minutes in TBS-T. The secondary antibody was diluted 1:2000 in blocking buffer. The membranes were then incubated in secondary antibody for 1 hour at room temperature on a shaker. After the incubation the membranes were washed in TBS-T three times for 10 minutes again.

The components of the Clarity Western ECL substrate were mixed at a ratio of 1:1 and the membranes were incubated in the substrate for 5 minutes. Then they were transferred between two clean sheets of foil. The chemiluminescence signal was visualised using the imaging platform Fusion FX (Vilber, France).

3. Results

3.1. Genotyping of MMTV-HA-Ovol1 mice

Since this project concerned the characterisation of mice harbouring the MMTV-HA-Ovol1 transgene, it was necessary to determine whether a mouse carried the transgenic allele. For genotyping tissue from ear notches was used and genotyping for the transgene was done by PCR.

The PCR for the transgenic allele amplifies a fragment with a length of 493 bp, while the corresponding *Ovol1* wildtype fragment is much longer (2602 bp when using the primer pair to detect the transgene allele). A PCR protocol with a short extension time was chosen to detect the transgenic allele. With this protocol only the transgenic fragment but not the wildtype fragment should be amplified (Fig. 6A). However, a 2.6 kb band corresponding to the band for the *Ovol1* wildtype allele was often observed in non-transgenic samples. To proof that the samples used in the study contain amplifiable genomic DNA, a second PCR with another primer pair located in the second intron of the *Ovol1* gene was performed (length of the fragment: 394 bp) (Fig. 6B).

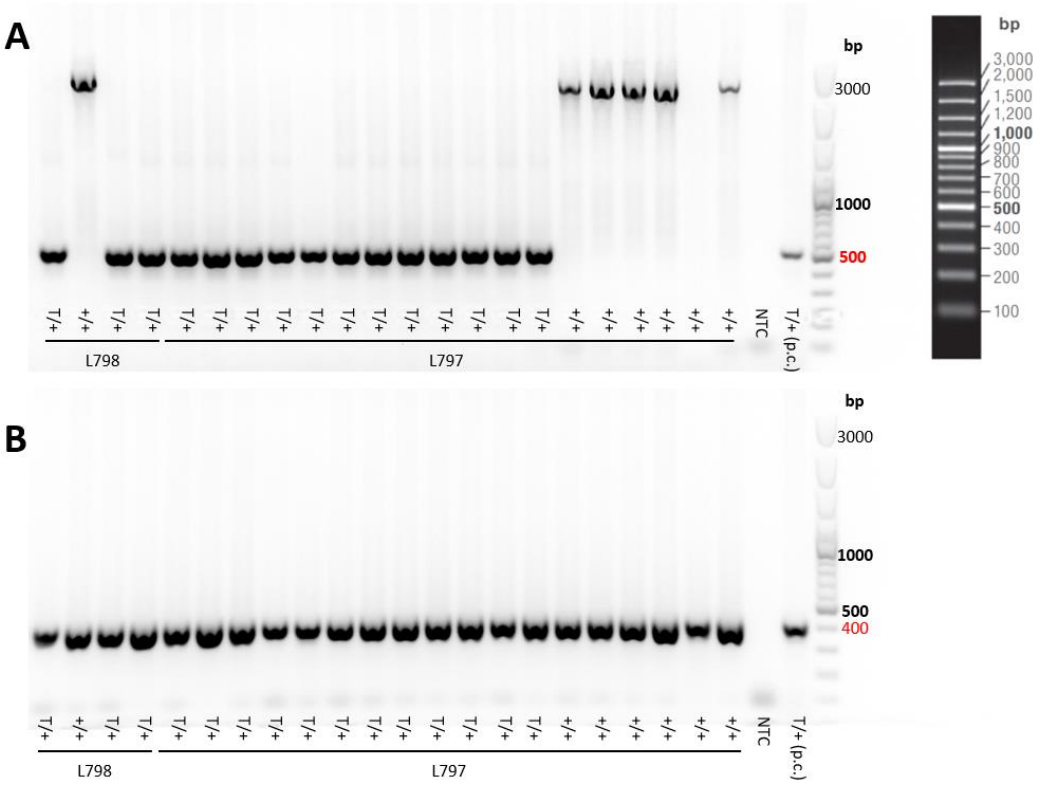

Figure 6: Representative MMTV-HA-Ovol1 genotyping PCR; DNA from a founder mouse was used as a positive control, the genotype assigned to each sample is shown below the gel (T/+ indicates the animal was transgenic, +/+ indicates a wildtype animal); A) samples tested for the transgene (493 bp), B) to test the amplification ability of the samples showing no band in A), a different assay amplifying a fragment of genomic DNA present in wildtype and transgenic animals was used (primer sequences see Tab. 1); PCR fragments were separated on a 1 % agarose gel; 100 bp plus Ladder was used to determine the fragment size. NTC – no template control, p.c. – positive control.

3.2. *Ovol1* expression analysis in different tissues by RT-PCR

The aim of the study was the generation of mice with increased expression of *Ovol1* in the mammary gland. Therefore, it was necessary to know, whether *Ovol1* expression can be detected in mammary gland tissue at all. As it is possible that the transgene is ectopically expressed in other tissues as well, it is also important to know the *Ovol1* expression levels in other tissues. For these reasons RT-PCR for *Ovol1* and the reference gene *Oaz1* on a panel of tissue samples prepared from wildtype mice was done. The results of these analyses are shown in Fig. 7.

The highest *Ovol1* expression was detected in kidney, testis and lung. The high expression levels in kidney and testis correlate well with previously published results (Dai et al., 1998; Li et al., 2005). *Ovol1* expression in skin could also be detected, whereas there was no measurable *Ovol1* expression in liver, heart, spleen and brain tissues. *Ovol1* expression in

mammary glands was detectable but seems to be rather low. Comparable levels of *Oaz1* were detected in all tissue samples.

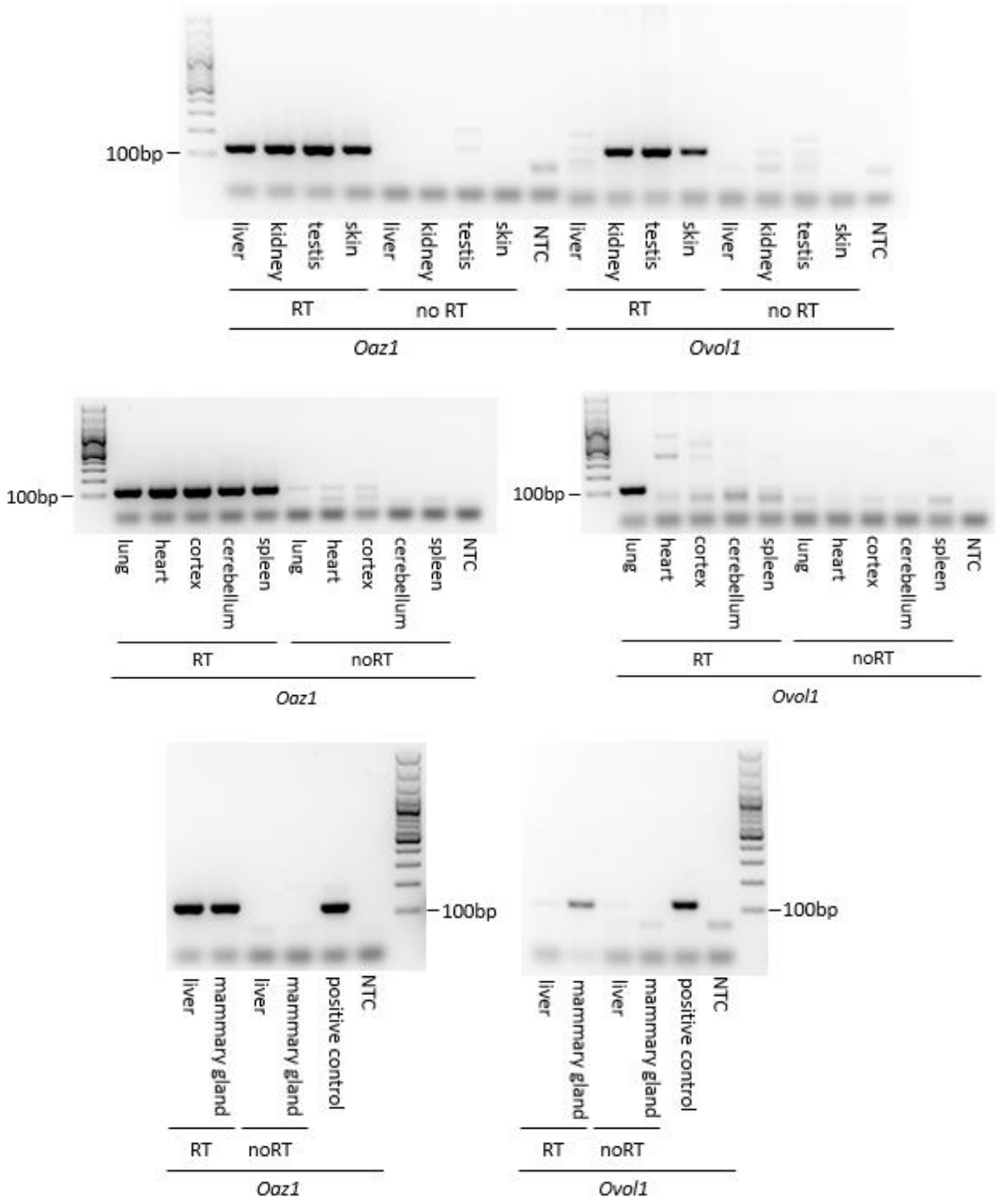

Figure 7: Tissue specific Ovol1 expression. RT-PCR for Ovol1 was performed on tissue samples from wildtype mice. Oaz1 was used as reference gene. After RT-PCR samples were loaded on a 2 % agarose gel and gel electrophoresis was performed. The 100 bp plus Ladder (Thermo Fisher Scientific) was used to determine the fragment size; NTC – no template control.

3.3. Selection of experimental animals

Transgenic animals generated by pronuclear injection often have multiple integrations of the transgene in different sites of the genome, which are independently transmitted to their offspring. Mice with different numbers of transgene integrations will also show differences in transgene expression levels and cannot be used for experiments. It is therefore necessary to identify mice with a stable transgene integration in only one genomic locus. Identification of stable transgenic lines was done according to the following approach. Transgenic male mice were mated to wildtype C57BL/6N females. In the case of a stable transgene integration half of the offspring should be transgenic. Higher numbers of transgenic offspring indicate that there is more than one transgene integration present in the genome of the father and these multiple integrations need to be separated by further breeding. The transgene transmission rate is an indicator but not proof for the presence of a stable integration.

Two males from L796, six males from L797 and four males from L798 were backcrossed to C57BL/6N females. The pups from these mating pairs were genotyped and the number of transgenic offspring counted.

Five males (L797_#17, L797_#22, L797_#40, L797_#50, L798_#49) sired transgenic pups at approximately the expected ratio of 50 % and were further evaluated. The offspring of the remaining males was not included in further experiments, because they transmitted the transgene at higher frequency to their offspring.

From each of the backcrosses four transgenic female mice were selected for *Ovol1* gene expression analysis. In addition several wildtype littermate control females were also chosen for gene expression analysis (for a list of mice see Supplementary Data, Table 16). Tissue samples from the mammary gland and other organs were prepared from these females as described in the methods section.

3.4. Ovol1 expression analysis in MMTV-HA-Ovol1 transgenic animals by RT-qPCR

In the first part of this work mice with an integration of the MMTV-HA-Ovol1 transgene in their genome were identified by conventional PCR. The expression levels of a transgene are influenced by several factors such as transgene copy number and locus of integration and may vary considerably between separate transgenic lines. To identify a line with high transgene

expression it is necessary to quantify the amount of transgene expression in the tissue of interest.

To screen for *Ovol1* expression in mammary glands RT-qPCRs were performed. RT-qPCR offers the advantage, that it is a sensitive and specific method for gene expression analysis and that many samples can be tested in one approach.

For RT-qPCR RNA was prepared from abdominal mammary glands and transcribed into cDNA. qPCR was performed to quantify the expression level of *Ovol1* compared to the reference genes *B2m* and *Oaz1*. The efficiency of the qPCR reactions for all three genes was tested in a small-scale approach and they performed within the predefined acceptability criteria described in the Methods section. Exemplary standard curves are shown in Fig. 8.

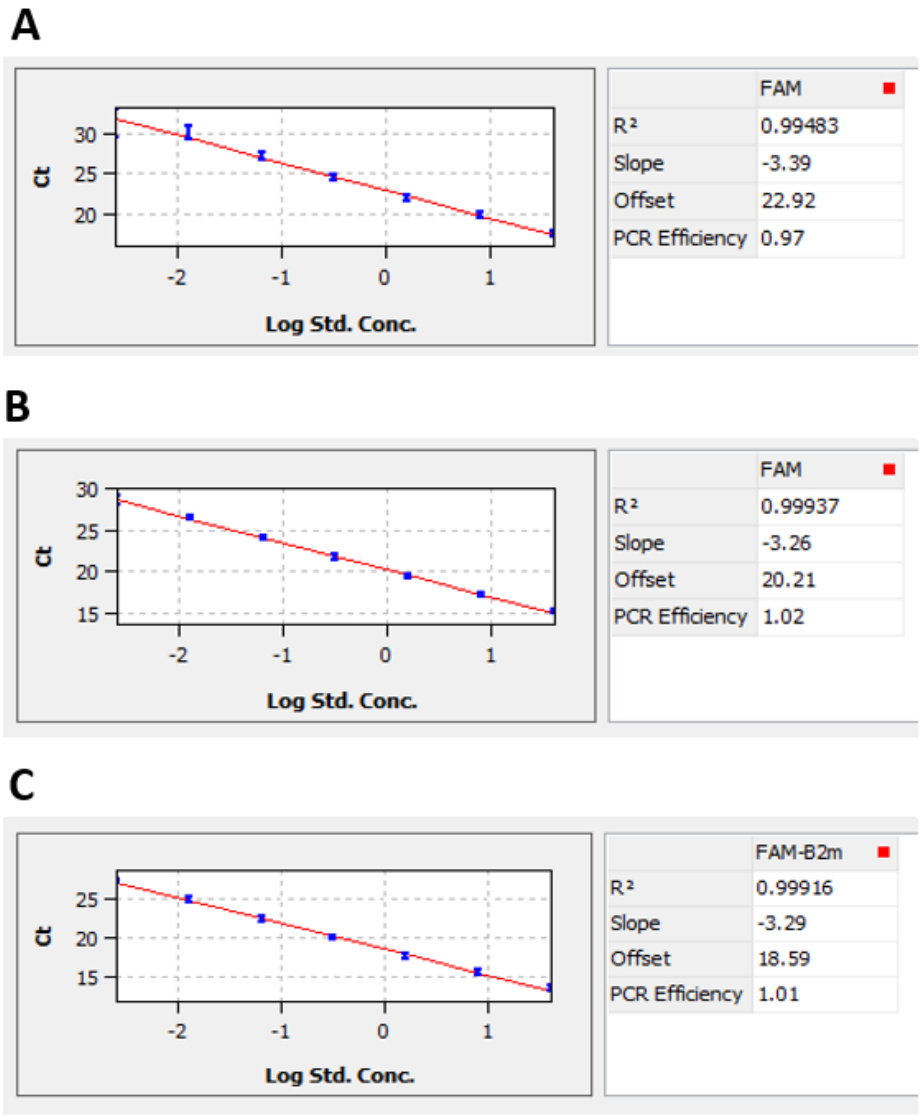

Figure 8: Standard curves of the performed RT-qPCRs for the genes Ovol1 (A), Oaz1 (B) and B2m (C); The RT-qPCR showed a good Efficiency with values between 97 % and 102 %, R^2 was > 0.99.

The offspring of four males was selected for *Ovol1* expression analysis by RT-qPCR. The results of this experiment are shown in Fig. 9.

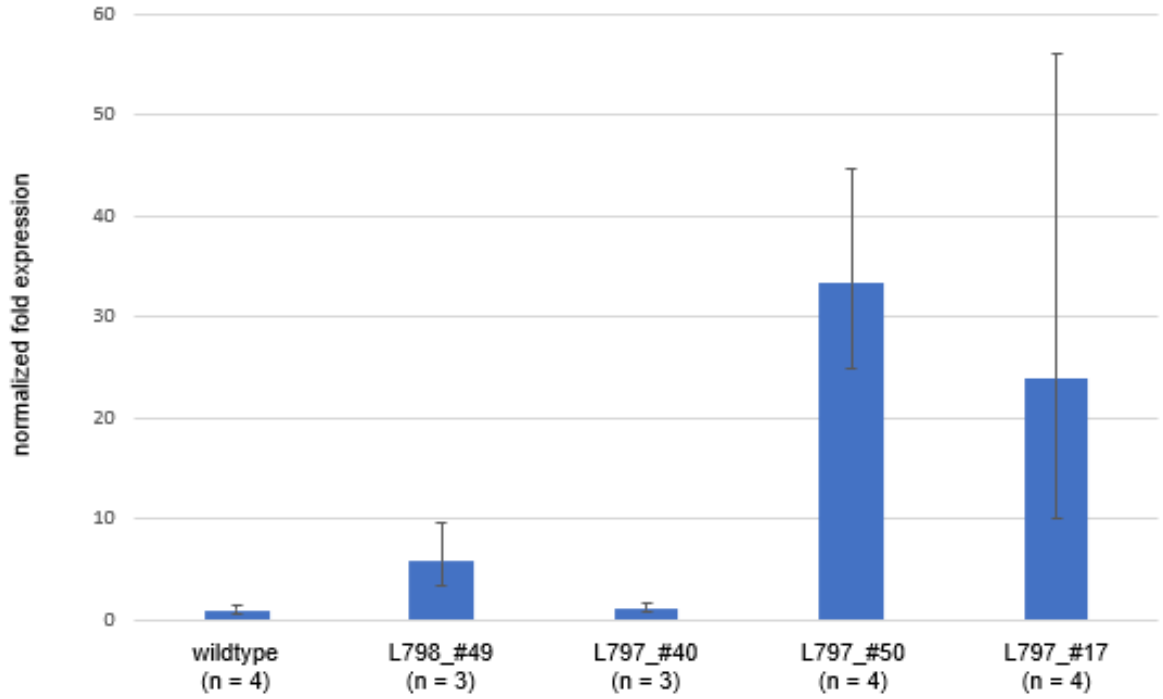

Figure 9: RT-qPCR analysis of Ovol1 expression in MMTV-HA-Ovol1 transgenic mice. Mice are grouped according to the subline. Ovol1 expression war normalized to the reference genes B2m and Oaz1. Ovol1 expression in transgenic lines is calculated in relation to the wildtype Ovol1 expression levels. Data are shown as average relative normalized expression ± SEM. The number of females evaluated is indicated. n – number of animals.

As expected from the RT-PCR experiment there is little *Ovol1* expression in mammary glands of wildtype mice. No increase in *Ovol1* expression could be detected in the mammary glands of subline L797_#40. A small increase in *Ovol1* expression was found in subline L798_#49. The most promising subline is L797_#50 which shows an approximately 30-fold *Ovol1 over*expression compared to the wildtype tissue. Subline 797_#17 also exhibits increased *Ovol1* expression, but there are some differences in *Ovol1* expression between the samples.

To ensure that the results of the RT-qPCR were not confounded by incorrectly genotyped mice, all animals used in this experiment were re-genotyped. Genotypes were confirmed for all animals except for one mouse, which could not be confirmed as transgenic.

3.5. Analysis of OVOL1 expression in MMTV-HA-Ovol1 transgenic mice

Since the increased transcription of a gene does not necessarily correlate with elevated protein expression, it is necessary to show that higher OVOL1 levels can be detected in the mammary glands of MMTV-HA-Ovol1 transgenic mice. To confirm HA-OVOL1 expression Western Blot

analysis was performed using an antibody recognizing the HA-Tag. With this antibody the HA-tagged but not the endogenous OVOL1 will be detected.

First, a Western Blot was performed to test the anti-HA antibody and to choose a positive control for further experiments. Three cell lysates that had been generated for other projects were tested. One cell lysate was from a HEK293 cell line expressing ING3 with a N-terminal HA-Tag (NHA-Ing3) and one sample was from a HEK293 cell line expressing C-terminally tagged ING3 (CHA-Ing3). The third sample, generated from NIH3T3 cells, expressed LRIG2. A cell lysate from untransfected HEK293 cells was used as control (Fig. 10).

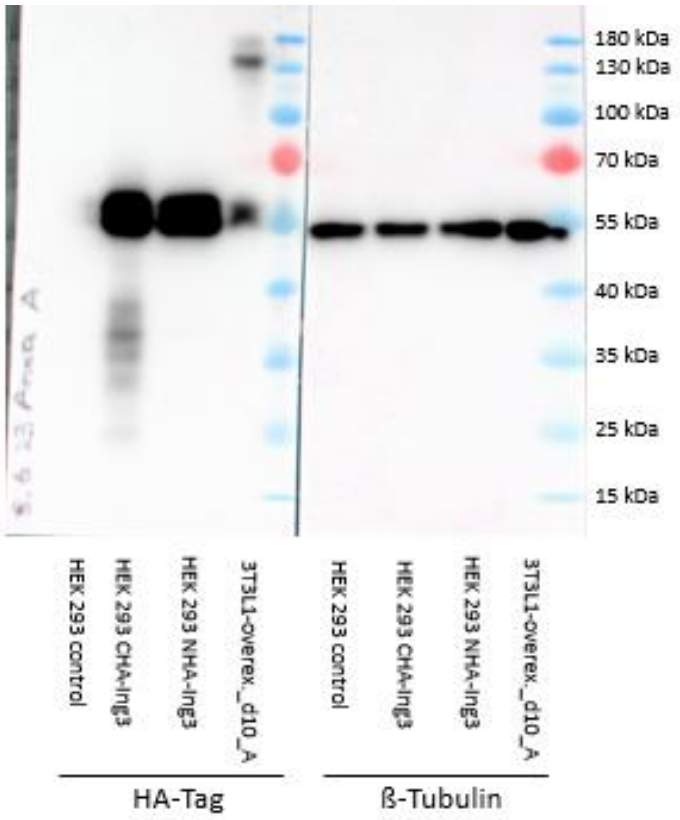

Figure 10: Western Blot analysis of HA-tagged cell lysates. The left half of the membrane was incubated with HA-Tag (C29F4) mAb to detect the HA-Tag and the right half was incubated with β-Tubulin mAb as reference antibody. A band at the expected height of 55kDa and 130kDa was detected for the ING3 and the LRIG2 expressing lysates respectively. The reference antibody detected a band at the expected height of 55kDa. Membranes were exposed for 1 minute.

All tested positive controls worked well. The sample HEK 293 NHA-Ing3 was chosen as positive control for further experiments. NHA-Ing3 has an N-terminal HA-Tag as does the *Ovol1* construct. Additionally, with 55 kDa ING3 is close to the size of OVOL1 which is about 35 kDa.

Next, the MMTV-HA-Ovol1 transgenic mice were tested by the Western Blot. Animals were chosen according to the results of the qPCR. Abdominal mammary gland protein lysates from four animals belonging to two high expressing lines, two to a low expressing line and two wildtype animals were tested by Western Blot. The positive control HEK 293 NHA-Ing3 was diluted 1:10 since the previous Western Blot showed a very high expression of the HA-tagged protein in this sample.

Transfer efficiency of the blot was evaluated by Ponceau S staining. Ponceau S staining showed that the transfer worked well, although larger proteins seem to have more efficiently transferred than smaller proteins (Fig. 11). For the positive control almost no bands are visible because this sample was diluted and the amount of protein loaded was very low.

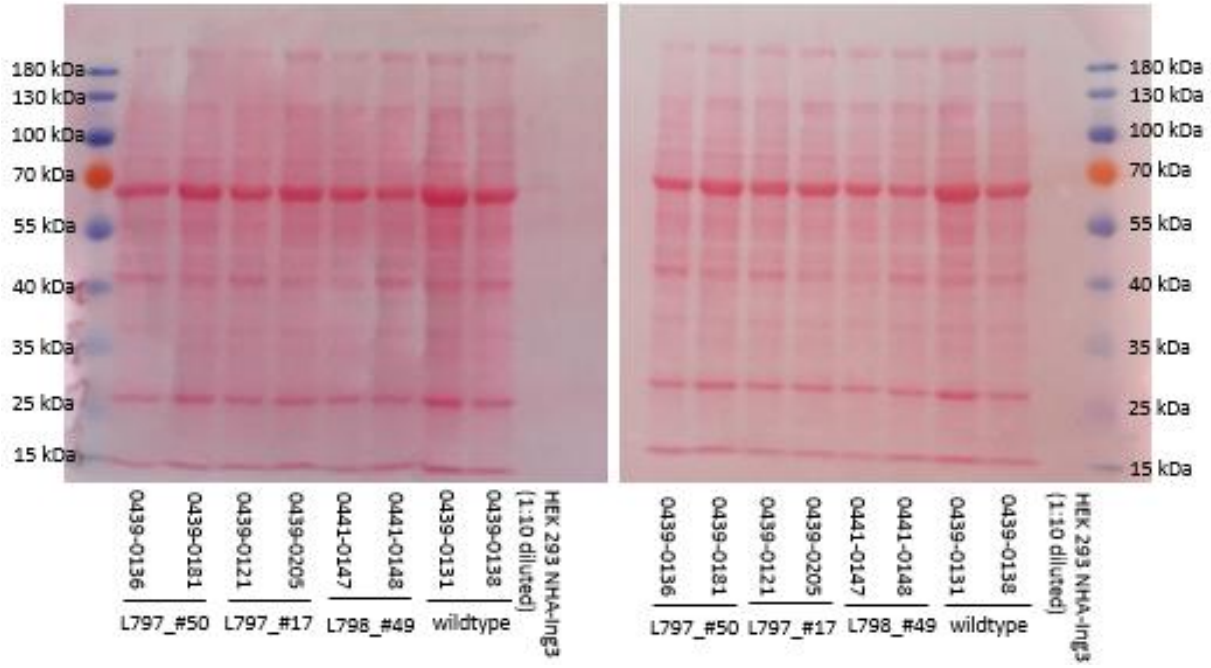

Figure 11: Ponceau S staining of the membranes used in the following Western Blot.

Membranes then again were incubated in primary and secondary antibodies (Fig. 12). The membrane incubated with β-Tubulin showed clear bands at 55 kDa even when exposed for a short time (1 minute). In contrast, the membrane incubated in HA-Tag antibody showed no bands around 35 kDa, where the band for the HA-tagged OVOL1 would be expected, even when the membrane was incubated for 20 minutes. The bands that can be seen at the top of the blot resulted from unspecific binding of the antibody.

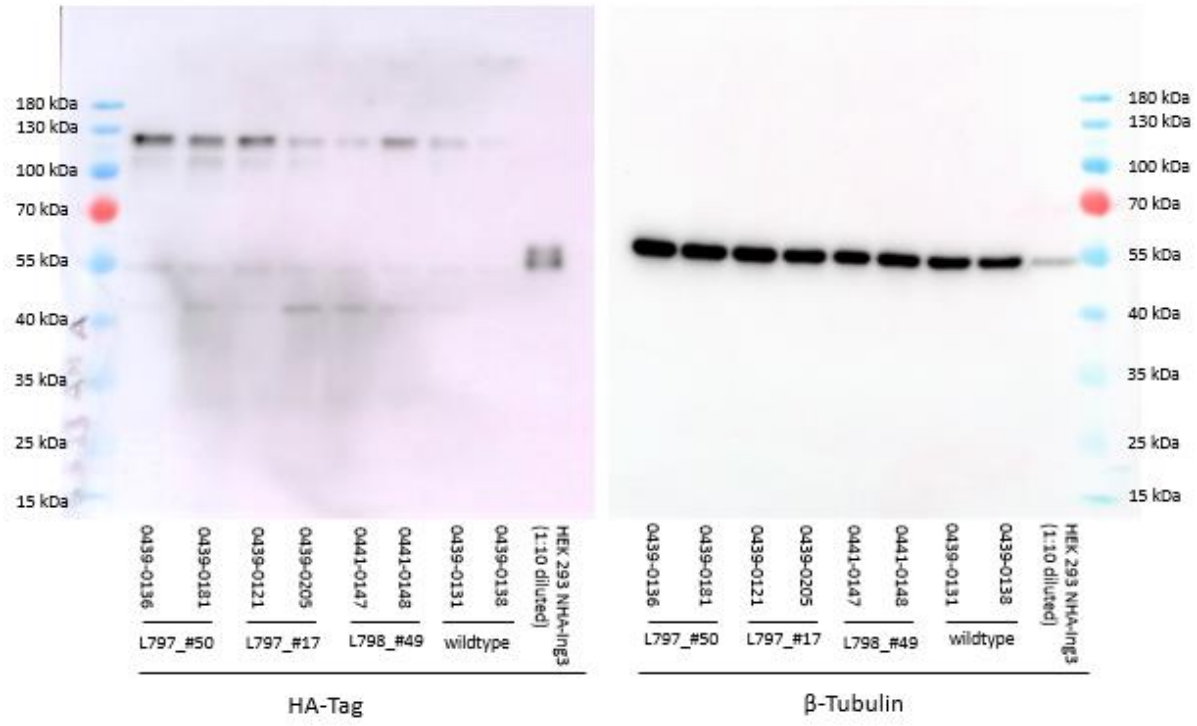

Figure 12: Western Blot to detect HA-OVOL1 expression in mammary glands from transgenic mice. 10 µg protein were loaded for each mammary gland sample, 2 µg protein was loaded for the positive control. The right membrane was incubated with β-Tubulin antibody as loading control. The left membrane was incubated with the HA-Tag antibody. The band for the HA-tagged OVOL1 should be visible at 35 kDa. The β-Tubulin and the HA-tag blots were exposed for one and 20 minutes respectively.

In the Western Blot described above, HA-tagged OVOL1 protein could not be detected in any of the protein lysates. The reasons for this need to be investigated in the future.

In addition, an antibody recognizing OVOL1 itself was tested in Western Blot. To test the OVOL1-antibody protein lysates from various tissues were used that should differ regarding their OVOL1 expression level. Kidney and testis samples were included, because they showed high *Ovol1* expression in the RT-PCR and OVOL1 expression in both tissues is described in the literature (Dai et al., 1998; Li et al., 2005). A liver sample was used, because according to the RT-PCR (Fig. 7) liver should show no OVOL1 expression. In addition, two mammary gland samples from a Ovol1 tissue specific knock-out mouse model were used. One of these samples is from a mouse with a mammary gland specific knock-out of *Ovol1*, while the other sample is from a control mouse. According to the RT-PCR data some OVOL1 expression in the mammary gland of the control mouse would be expected, but no OVOL1 expression in the mammary gland of the tissue specific knock-out mouse.

The membrane was cut in two pieces. The left part was incubated with the OVOL1 polyclonal antibody, the right part with the β-Tubulin antibody as loading control. As can be seen in Fig. 13 β-Tubulin showed a clear band at 55 kDa even at an exposure time of 1 minute. In contrast, on the left part no bands could be detected at the expected height of 35 kDa, whereas several bands with higher molecular weight appeared upon longer membrane exposure. These high molecular weight bands could be the result of extensive posttranslational modifications such as glycosylations, but no such posttranslational modifications have been reported for OVOL1 in the literature so far. The specificity of the antibody could be further investigated using tissue samples from a complete *Ovol1* knock-out mouse.

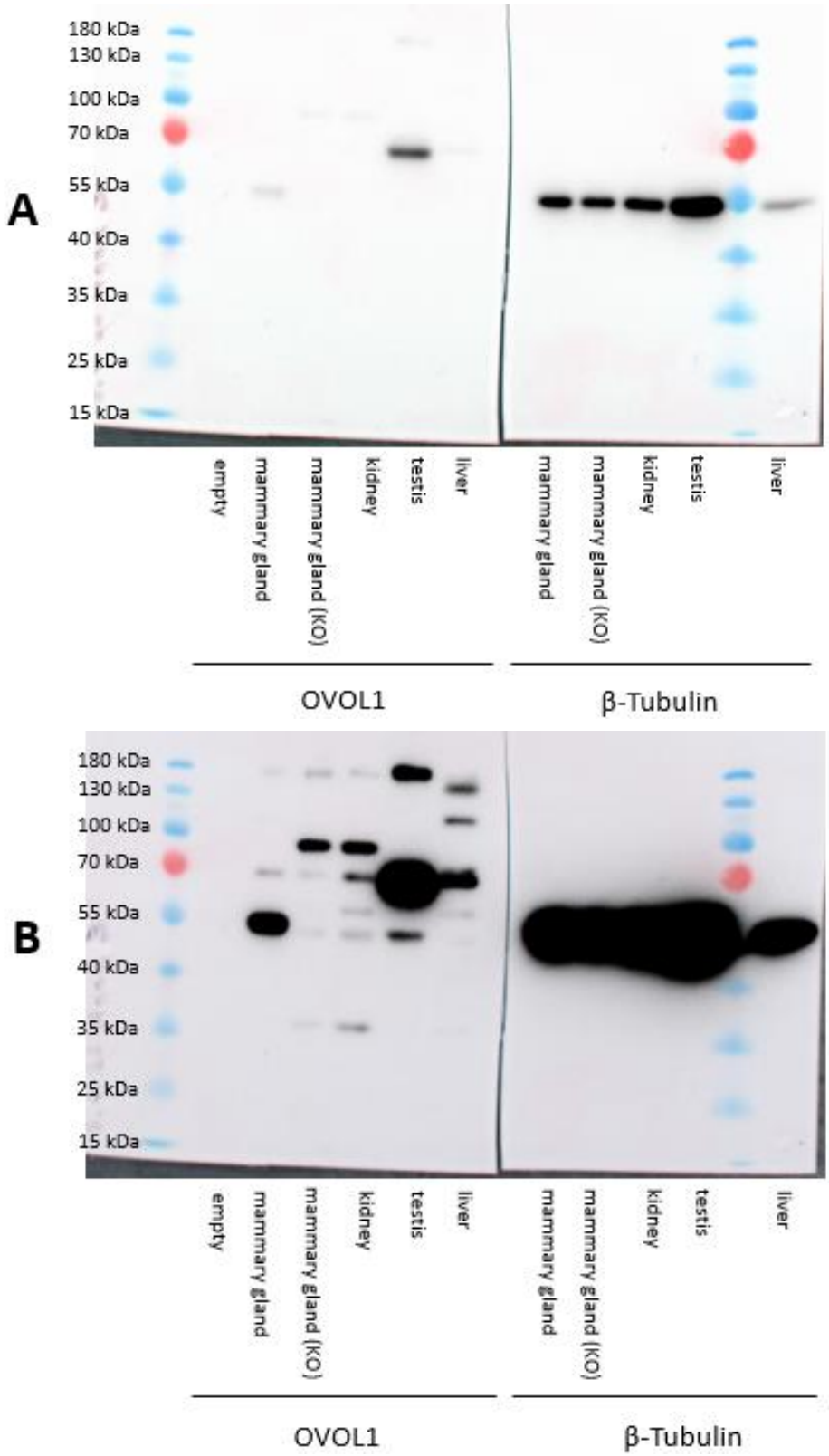

Figure 13: Western Blot for testing the OVOL1 antibody. β-Tubulin was used as loading control. Membranes were exposed for one minute (A) and 20 minutes (B). Mammary gland (KO) – mammary gland sample with a mammary gland specific-knock out of OVOL1.

4. Discussion

Understanding the mechanisms of cancer development is an important step in developing novel approaches for treating this disease. The transcription factor OVOL1 seems to play a role in the epithelial-mesenchymal plasticity of cancer cells. Further clarification of its function in these processes and identification of downstream targets may lead to the development of novel treatments for metastatic breast cancer.

Previous studies report varying OVOL1 expression in different tissue types. Expression was reported to be high in testis, kidney, skin and weakly in the lung, while expression in liver tissue was not detected (Dai et al., 1998; Li et al., 2005; Saxena et al., 2022). Using RT-PCR these findings could be confirmed. RT-PCR showed no expression of *Ovol1* in the liver tissue sample but clear expression in testis, kidney, lung and, though slightly less, skin. Dai et al. found *Ovol1* expression in the lung to be very weak, the RT-PCR in contrary showed an expression of *Ovol1* in the lung comparable with expression in kidney and testis (Fig. 7). *Ovol1* expression was also detected in the mammary gland, which had not been previously described.

The objective of this thesis was the characterisation of a novel mouse model overexpressing OVOL1 in mammary glands.

RT-qPCR was initially used to screen for *Ovol1* overexpression in transgenic sublines. Four sublines were included into the analysis (L797_#17, L797_#40, L797_#50 and L798_#49). L797_#40 did not show *Ovol1* expression above the wildtype level, while L797_#49 showed slightly increased *Ovol1* levels. The genotype of all animals used in the experiment was confirmed by PCR, excluding the possibility that the animals from the subline which only shows wildtype *Ovol1* expression level were wrongly genotyped. In this subline the transgene most probably integrated into a genomic locus that is not active in mammary gland tissue.

Two of the four sublines tested showed significantly increased *Ovol1* overexpression (L797_#50 and L797_#17). One of these overexpressing lines, line 797_#17, showed a quite high variability between the samples prepared from different animals. This variability may be due to several reasons.

Samples prepared from mammary glands are very heterogeneous since many different cell types are present in mammary gland tissue (Inman et al., 2015). These include the cells of the epithelial ductal network as such but also stromal cells such as fat cells from the surrounding fat pad, fibroblasts and immune cells. The basal and luminal cells of the ductal network both contain several subtypes of cells. The MMTV-promoter should only be active in luminal cells,

which are only a small fraction of the cells in mammary gland tissue. In the adult virgin mice used in this experiment, fat cells are the most abundant cells in the samples. Samples may differ in their cellular composition even when harvested from the same animal, which will lead to variable transgene expression levels.
In addition, transgene expression levels may be affected by the oestrous cycle of the mouse. The MMTV-promoter gets activated in response to the hormone progesterone (Beato et al., 2020). Fluctuations in progesterone levels during the oestrous cycle may cause changes in the activity of the MMTV-promoter and lead to higher or lower transcription of the transgene mRNA.
Another possibility for the observed variability in *Ovol1* expression levels in one of the *Ovol1* overexpressing sublines is, that there are two transgene integrations present in this line – one with a high transgene expression level and one with a lower. This should be avoided by only including sublines into the analysis, where transgene transmission occurred at the expected mendelian ratio of approximately 50 %, but cannot completely exclude the possibility of a second transgene integration. To test whether this is the case, females from this subline would have to be backcrossed for one more generation.

Confirmation of OVOL1 overexpression on protein level was performed by Western Blot analysis. The antibody of choice for this analysis was not directed against the OVOL1 protein itself, but against the HA-Tag present at the OVOL1 N-terminus.
Using an HA-Tag for detection is a widely used method. The suitability of the HA-tag antibody for this project was tested on cell lysates expressing different HA-tagged proteins. The antibody worked well since all positive controls showed a band at the expected height.

When mammary gland protein lysates from the MMTV-HA-Ovol1 high expressing sublines were tested using the strategy described above, no band was detected at the expected molecular weight for OVOL1. As these two lines show high *Ovol1* expression levels in the qPCR this result was unexpected. It remains to be investigated, why no HA-Tag could be detected in the tested transgenic MMTV-HA-Ovol1 mice. A combination of several factors may be responsible for this unsuccessful attempt at detecting HA-tagged OVOL1.

Owing to the previously discussed heterogeneity of the mammary gland tissue the transgene should only be expressed in a subset of mammary gland cells (luminal cells) and the tissue sample could only contain a relatively low amount of OVOL1. It may be necessary to use a higher amount of protein lysate for Western Blot analysis.

The problem with OVOL1 detection could be related to suboptimal blotting conditions. As can be seen in Ponceau S staining (Fig. 11), bands around 35 kDa, where OVOL1 is supposed to be, were very light, while transfer of larger proteins worked much better. A long transfer time may allow smaller proteins to pass through the membrane onto the filter paper leaving light or even no bands on the membrane (Bass et al., 2017; Kurien & Hal Scofield, 2015). The transfer program was chosen in accordance with the manual of the blotting device. In future experiments blotting conditions need to be optimised to allow efficient transfer of smaller proteins.

An antibody against OVOL1 on different mouse tissue samples was tested. This antibody had been successfully used to detect human OVOL1 (Roca et al., 2013) and was described as suitable for detecting mouse OVOL1. The samples were chosen according to the RT-PCR and published results and included samples with high and low *Ovol1* expression levels. No bands were detected at the expected height for OVOL1 (Fig. 13), indicating that Western Blot conditions for this antibody need to be optimised. For optimisation of these conditions a suitable negative control must be included such as a knock-down (KD) cell lysate or a tissue sample from a complete knock-out (KO) mouse.

In the course of this bachelor thesis, two MMTV-HA-Ovol1 transgenic sublines were identified that overexpress *Ovol1*. More analyses will be needed to confirm the suitability of these lines for their intended use in cancer research.

5. Summary

Breast cancer is one of the most common cancers in females. Treatment options have improved over the last years but are still often not successful, in many cases due to the formation of metastasis.

Recent studies suggest that the transcription factor OVOL1 (ovo like zinc finger 1) may play a role in the epithelial-mesenchymal plasticity of cancer cells.

To further investigate the role of OVOL1 in mammary gland tumours it is crucial to create suitable animal models. A mouse model expressing mammary gland specific OVOL1 was developed at the Institute of *in vivo* and *in vitro* Models. Therefore, a construct consisting of the haemagglutinin (HA)-tagged coding sequence of *Ovol1* controlled by the Mouse Mammary Tumour Virus (MMTV) promoter was cloned (MMTV-HA-Ovol1).

Three MMTV-HA-Ovol1 transgenic founder lines were established. Pups were genotyped by PCR. Transgenic and wildtype female mice from each line were sacrificed and tissue samples were harvested from each mouse to prepare RNA and protein lysates.

Reverse transcriptase quantitative PCR (RT-qPCR) was applied to assess differences in transgene expression in separate transgenic sublines. qPCR assays for *Ovol1* and two reference genes (*Oaz1* (Ornithine decarboxylase antizyme 1) and *B2m* (Beta-2 microglobulin)) were set up and tested. RNA was prepared from abdominal mammary gland samples and complementary DNA was synthesised for measuring *Ovol1* expression using RT-qPCR and quantifying it using *Oaz1* and *B2m* for normalisation. Two sublines with significantly increased *Ovol1* transcription were identified.

Western Blot analysis was performed to confirm expression of the HA-OVOL1 protein. An anti-HA antibody was used to detect OVOL1 in the two overexpressing sublines. Suitability of the anti-HA antibody was confirmed by testing it on protein lysates from cells overexpressing different HA-tagged proteins. It was not possible to detect OVOL1 in mammary glands of transgenic mice using the initial approach but may be feasible upon improvement of Western Blot conditions.

6. Zusammenfassung

Brustkrebs ist eine der häufigsten Krebsarten bei Frauen. Die Behandlung hat sich in den letzten Jahren verbessert, ist aber immer noch oft nicht erfolgreich, nicht zuletzt aufgrund der häufigen Entstehung von Metastasen.

Aktuelle Studien deuten darauf hin, dass der Transkriptionsfaktor OVOL1 (ovo like zinc finger 1) eine Rolle bei der epithelial-mesenchymalen Transition spielen könnte.

Um die Rolle von OVOL1 bei Brustkrebs weiter untersuchen zu können, müssen geeignete Tiermodelle generiert werden. Daher wurde am Institut für *In-vivo* und *In-vitro*-Modelle ein Mausmodell entwickelt, das OVOL1 in der Brustdrüse überexprimiert. Der cDNA von *Ovol1* wurde ein Hämagglutinin (HA)-Tag angehängt und unter die Kontrolle des „Mouse Mammary Tumour Virus“ (MMTV)-Promotors gesetzt, an die cDNA wurde abschließend ein SV40-Polyadenylisierungssignal angehängt (MMTV-HA-Ovol1).

Es wurden drei transgene MMTV-HA-Ovol1-Mauslinien erstellt, deren Nachkommen mittels PCR genotypisiert wurden. Weibliche transgene Tiere und nicht transgene Wurfgeschwister wurden euthanasiert und ihnen wurde Gewebe entnommen. Aus diesen Gewebeproben wurde RNA isoliert und Proteinlysate wurden hergestellt.

Eine Quantitative Reverse-Transkriptase-PCR (RT-qPCR) wurde verwendet, um Unterschiede in der Transgenexpression in den einzelnen transgenen Sublinien zu untersuchen. qPCR-Assays für *Ovol1* und zwei Referenzgene (*Oaz1* (Ornithindecarboxylase-Antizym 1) und *B2m* (Beta-2-Mikroglobulin)) wurden erstellt und analysiert. Aus Proben der abdominalen Milchdrüse wurde RNA isoliert und komplementäre DNA synthetisiert, um die Expression von *Ovol1* mittels RT-qPCR zu messen und sie anhand von *Oaz1* und *B2m* zu quantifizieren. Es konnten zwei Sublinien mit signifikant erhöhter *Ovol1*-Transkription identifiziert werden.

Western-Blot-Analysen wurden durchgeführt, um in den Sublinien mit erhöhter *Ovol1* Transkription auch OVOL1 auf Proteinebene nachzuweisen. Dafür wurde ein gegen das HA-Tag gerichteter Antikörper verwendet. Als Positivkontrolle wurden Proteinlysate von Zellen verwendet, die verschiedene mit HA-Tag markierte Proteine überexprimieren. Bei den ersten Analysen konnte keine OVOL1 Expression in der Brustdrüse transgener Mäuse nachgewiesen werden, aber eine Optimierung der Western Blot Bedingungen sollte die Detektion des Transgens ermöglichen.

7. List of Abbreviations

B2m	*Beta-2-microglobulin*
bp	Base pairs
BSA	Bovine Serum Albumin
cDNA	Complementary DNA
CDS	Coding sequence
CHA	C-terminally tagged
Cq	Cycle threshold
EMT	Epithelial-mesenchymal-transition
HA	Haemagglutinin
HEK	Human embryonic kidney
ING3	Inhibitor Of Growth Family Member 3
KD	Knock-down
KO	Knock-out
LRIG2	Leucine Rich Repeats And Immunoglobulin Like Domains 2
MET	Mesenchymal-epithelial-transition
MMTV	Mouse Mammary Tumour Virus
NHA	N-terminally tagged
NLS	Nuclear localisation site
NTC	No template control
Oaz1	*Ornithine decarboxylase antizyme 1*
Ovol1	*Ovo-like zinc finger 1*
poly A	Polyadenylation
PVDF	Polyvinyliden fluorid
qRT-PCR	quantitative reverse transcriptase PCR
SV40	Simian Virus 40
TEBs	Terminal End Buds

8. References

Allen, N. D., Norris, M. L., & Surani, M. A. (1990). Epigenetic Control of Transgene Expression and Imprinting by Genotype-Specific Modifiers. *Cell*, *61*(5), 853–861. https://doi.org/10.1016/0092-8674(90)90195-k

Bass, J. J., Wilkinson, D. J., Rankin, D., Phillips, B. E., Szewczyk, N. J., Smith, K., & Atherton, P. J. (2017). An overview of technical considerations for Western blotting applications to physiological research. *Scandinavian Journal of Medicine and Science in Sports*, *27*(1), 4–25. https://doi.org/10.1111/sms.12702

Beato, M., Wright, R. H. G., & Le Dily, F. (2020). Molecular mechanisms of progesterone receptor action on the breast cancer genome. *Journal of Molecular Endocrinology*, *65*(1), T65–T79. https://doi.org/10.1530/JME-19-0266

Boman, C., Edman Kessler, L., Bergh, J., Matikas, A., & Foukakis, T. (2022). Women with short survival after diagnosis of metastatic breast cancer: a population-based registry study. *Breast Cancer Research and Treatment*, *194*(1), 49–56. https://doi.org/10.1007/s10549-022-06591-7

Chaffer, C. L., Brennan, J. P., Slavin, J. L., Blick, T., Thompson, E. W., & Williams, E. D. (2006). Mesenchymal-to-epithelial transition facilitates bladder cancer metastasis: Role of fibroblast growth factor receptor-2. *Cancer Research*, *66*(23), 11271–11278. https://doi.org/10.1158/0008-5472.CAN-06-2044

Dai, X., Schonbaum, C., Degenstein, L., Bai, W., Mahowald, A., & Fuchs, E. (1998). The ovo gene required for cuticle formation and oogenesis in flies is involved in hair formation and spermatogenesis in mice. *Genes & Development*, *12*(21), 3452–3463. https://doi.org/10.1101/gad.12.21.3452

dos Santos, C. O., Dolzhenko, E., Hodges, E., Smith, A. D., & Hannon, G. J. (2015). An Epigenetic Memory of Pregnancy in the Mouse Mammary Gland. *Cell Reports*, *11*(7), 1102–1109. https://doi.org/10.1016/j.celrep.2015.04.015

Elder, A. M., Tamburini, B. A. J., Crump, L. S., Black, S. A., Wessells, V. M., Schedin, P. J., Borges, V. F., & Lyons, T. R. (2018). Semaphorin 7A promotes macrophage-mediated lymphatic remodeling during postpartum mammary gland involution and in breast cancer. *Cancer Research*, *78*(22), 6473–6485. https://doi.org/10.1158/0008-5472.CAN-18-1642

Ferlay, J., Ervik, M., Colombet, M., Mery, L., Piñeros, M., Znaor, A., Soerjomataram, I., & Bray, F. (n.d.). *Global Cancer Observatory: Cancer Today. Lyon, France: International Agency for Research on Cancer*. https://gco.iarc.fr/today/online-analysis. Accessed 15/07/2023

García-Gutiérrez, L., Delgado, M. D., & León, J. (2019). Myc oncogene contributions to release of cell cycle brakes. *Genes*, *10*(3). https://doi.org/10.3390/genes10030244

Honvo-Houéto, E., & Truchet, S. (2015). Indirect immunofluorescence on frozen sections of mouse mammary gland. *Journal of Visualized Experiments*, *106*. https://doi.org/10.3791/53179

Inman, J. L., Robertson, C., Mott, J. D., & Bissell, M. J. (2015). Mammary gland development: Cell fate specification, stem cells and the microenvironment. *Development*, *142*(6), 1028–1042. https://doi.org/10.1242/dev.087643

Jolly, M. K., Jia, D., Boareto, M., Mani, S. A., Pienta, K. J., Ben-Jacob, E., & Levine, H. (2015). Coupling the modules of EMT and stemness: A tunable “stemness window” model. *Oncotarget*, *6*(28), 25161–25174. https://doi.org/10.18632/oncotarget.4629

Kurien, B. T., & Hal Scofield, R. (2015). Western blotting: An introduction. In *Western Blotting: Methods and Protocols* (Vol. 1312, pp. 17–30). Springer New York. https://doi.org/10.1007/978-1-4939-2694-7_5

Li, B., Mackay, D. R., Dai, Q., H Li, T. W., Nair, M., Fallahi, M., Schonbaum, C. P., Fantes, J., Mahowald, A. P., Waterman, M. L., Fuchs, E., & Dai, X. (2002). The LEF1/β-catenin complex activates movo1, a mouse homolog of Drosophila ovo required for epidermal appendage differentiation. *Proc Natl Acad Sci U S A*, *99*(9), 6064–6069. https://doi.org/10.1073/pnas.092137099

Li, B., Nair, M., Mackay, D. R., Bilanchone, V., Hu, M., Fallahi, M., Song, H., Dai, Q., Cohen, P. E., & Dai, X. (2005). Ovol1 regulates meiotic pachytene progression during spermatogenesis by repressing Id2 expression. *Development*, *132*(6), 1463–1473. https://doi.org/10.1242/dev.01658

Maajani, K., Jalali, A., Alipour, S., Khodadost, M., Tohidinik, H. R., & Yazdani, K. (2019). The Global and Regional Survival Rate of Women With Breast Cancer: A Systematic Review and Meta-analysis. *Clinical Breast Cancer*, *19*(3), 165–177. https://doi.org/10.1016/j.clbc.2019.01.006

Mähler, M., Berar, M., Feinstein, R., Gallagher, A., Illgen-Wilcke, B., Pritchett-Corning, K., & Raspa, M. (2014). FELASA recommendations for the health monitoring of mouse, rat, hamster, guinea pig and rabbit colonies in breeding and experimental units. *Laboratory Animals*, *48*(3), 178–192. https://doi.org/10.1177/0023677213516312

Nair, M., Teng, A., Bilanchone, V., Agrawal, A., Li, B., & Dai, X. (2006). Ovol1 regulates the growth arrest of embryonic epidermal progenitor cells and represses c-myc transcription. *Journal of Cell Biology*, *173*(2), 253–264. https://doi.org/10.1083/jcb.200508196

Roca, H., Hernandez, J., Weidner, S., McEachin, R. C., Fuller, D., Sud, S., Schumann, T., Wilkinson, J. E., Zaslavsky, A., Li, H., Maher, C. A., Daignault-Newton, S., Healy, P. N., & Pienta, K. J. (2013). Transcription Factors OVOL1 and OVOL2 Induce the Mesenchymal to Epithelial Transition in Human Cancer. *PLoS ONE*, *8*(10). https://doi.org/10.1371/journal.pone.0076773

Rülicke, T., & Hübscher, U. (2000). Germ line transformation of mammals by pronuclear microinjection. *Experimental Physiology*, *85*(6), 589–601. https://doi.org/10.1111/j.1469-445X.2000.02092.x

Saxena, K., Srikrishnan, S., Celia-Terrassa, T., & Jolly, M. K. (2022). OVOL1/2: Drivers of Epithelial Differentiation in Development, Disease, and Reprogramming. *Cells Tissues Organs*, *211*(2), 183–192. https://doi.org/10.1159/000511383

Taneja, P., Frazier, D. P., Kendig, R. D., Maglic, D., Sugiyama, T., Kai, F., Taneja, N. K., & Inoue, K. (2009). MMTV mouse models and the diagnostic values of MMTV-like sequences in human breast cancer. *Expert Review of Molecular Diagnostics*, *9*(5), 423–440. https://doi.org/10.1586/erm.09.31

Taylor, S. C., Nadeau, K., Abbasi, M., Lachance, C., Nguyen, M., & Fenrich, J. (2019). The Ultimate qPCR Experiment: Producing Publication Quality, Reproducible Data the First Time. In *Trends in Biotechnology* (Vol. 37, Issue 7, pp. 761–774). Elsevier Ltd. https://doi.org/10.1016/j.tibtech.2018.12.002

Wagner, K. U., Ward, T., Davis, B., Wiseman, R., & Hennighausen, L. (2001). Spatial and temporal expression of the Cre gene under the control of the MMTV-LTR in different lines of transgenic mice. *Transgenic Research*, *10*(6), 545–553. https://doi.org/10.1023/A:1013063514007

Wang, R., Zhu, Y., Liu, X., Liao, X., He, J., & Niu, L. (2019). The Clinicopathological features and survival outcomes of patients with different metastatic sites in stage IV breast cancer. *BMC Cancer*, *19*(1). https://doi.org/10.1186/s12885-019-6311-z

Wang, X., Spandidos, A., Wang, H., & Seed, B. (2012). PrimerBank: A PCR primer database for quantitative gene expression analysis, 2012 update. *Nucleic Acids Research*, *40*(D1), D1144–D1149. https://doi.org/10.1093/nar/gkr1013

Watson, C. J., & Khaled, W. T. (2008). Mammary development in the embryo and adult: A journey of morphogenesis and commitment. *Development*, *135*(6), 995–1003. https://doi.org/10.1242/dev.005439

Watson, C. J., & Khaled, W. T. (2020). Mammary development in the embryo and adult: New insights into the journey of morphogenesis and commitment. *Development*, *147*(22). https://doi.org/10.1242/dev.169862

Yang, J., & Weinberg, R. A. (2008). Epithelial-Mesenchymal Transition: At the Crossroads of Development and Tumor Metastasis. *Developmental Cell*, *14*(6), 818–829. https://doi.org/10.1016/j.devcel.2008.05.009

Zeng, L., Li, W., & Chen, C. S. (2020). Breast cancer animal models and applications. *Zoological Research*, *41*(5), 477–494. https://doi.org/10.24272/J.ISSN.2095-8137.2020.095

Zhao, W., & Méresse, S. (2015). A method to introduce an internal tag sequence into a salmonella chromosomal gene. In *Methods in Molecular Biology* (Vol. 1225, pp. 81–92). Humana Press Inc. https://doi.org/10.1007/978-1-4939-1625-2_5

9. Appendix

9.1. List of Tables and Figures

9.2. Supplementary Data

Table 18: Mice used for tissue preparation.

Mouse strain	Animal-ID	Gender	Genotype
MMTV-HA-Ovol1, L-797	0439-0003	female	T/+
MMTV-HA-Ovol1, L-797_#17	0439-0113	female	+/+
MMTV-HA-Ovol1, L-797_#17	0439-0121	female	T/+
MMTV-HA-Ovol1, L-797_#17	0439-0122	female	+/+
MMTV-HA-Ovol1, L-797_#17	0439-0199	female	T/+
MMTV-HA-Ovol1, L-797_#17	0439-0201	female	T/+
MMTV-HA-Ovol1, L-797_#19	0439-0131	female	+/+
MMTV-HA-Ovol1, L-797_#22	0439-0161	female	+/+
MMTV-HA-Ovol1, L-797_#22	0439-0257	female	+/+
MMTV-HA-Ovol1, L-797_#22	0439-0258	female	+/+
MMTV-HA-Ovol1, L-797_#22	0439-0259	female	T/+
MMTV-HA-Ovol1, L-797_#22	0439-0260	female	T/+
MMTV-HA-Ovol1, L-797_#22	0439-0261	female	T/+
MMTV-HA-Ovol1, L-797_#22	0439-0262	female	T/+
MMTV-HA-Ovol1, L-797_#22	0439-0263	female	+/+
MMTV-HA-Ovol1, L-797_#40	0439-0166	female	T/+
MMTV-HA-Ovol1, L-797_#40	0439-0167	female	T/+
MMTV-HA-Ovol1, L-797_#40	0439-0171	female	T/+
MMTV-HA-Ovol1, L-797_#40	0439-0172	female	T/+
MMTV-HA-Ovol1, L-797_#40	0439-0269	female	T/+
MMTV-HA-Ovol1, L-797_#40	0439-0270	female	T/+
MMTV-HA-Ovol1, L-797_#40	0439-0271	female	T/+
MMTV-HA-Ovol1, L-797_#40	0439-0272	female	T/+
MMTV-HA-Ovol1, L-797_#40	0439-0273	female	T/+
MMTV-HA-Ovol1, L-797_#40	0439-0274	female	+/+
MMTV-HA-Ovol1, L-797_#50	0439-0136	female	T/+
MMTV-HA-Ovol1, L-797_#50	0439-0138	female	+/+
MMTV-HA-Ovol1, L-797_#50	0439-0139	female	T/+
MMTV-HA-Ovol1, L-797_#50	0439-0180	female	T/+
MMTV-HA-Ovol1, L-797_#50	0439-0181	female	T/+
MMTV-HA-Ovol1, L-797_#50	0439-0205	female	T/+
MMTV-HA-Ovol1, L-797_#50	0439-0279	female	+/+
MMTV-HA-Ovol1, L-797_#50	0439-0280	female	T/+
MMTV-HA-Ovol1, L-797_#50	0439-0281	female	+/+
MMTV-HA-Ovol1, L-797_#50	0439-0282	female	+/+
MMTV-HA-Ovol1, L-797_#50	0439-0283	female	T/+
MMTV-HA-Ovol1, L-797_#50	0439-0284	female	T/+
MMTV-HA-Ovol1, L-797_#50	0439-0285	female	+/+
MMTV-HA-Ovol1, L-798_#28	0441-0071	female	+/+
MMTV-HA-Ovol1, L-798_#49	0441-0145	female	T/+

MMTV-HA-Ovol1, L-798_#49	0441-0146	female	+/+
MMTV-HA-Ovol1, L-798_#49	0441-0147	female	T/+
MMTV-HA-Ovol1, L-798_#49	0441-0148	female	T/+